SMHI

No 109, Feb 2006

Reports Meteorology and Climatology

Climate change scenario simulations of wind, sea level, and river discharge in the Baltic Sea and Lake Mälaren region – a dynamical downscaling approach from global to local scales

H.E. Markus Meier[1], Johan Andréasson[1], Barry Broman[1], L. Phil Graham[1], Erik Kjellström[1], Gunn Persson[1] and Michael Viehhauser[2]

[1]Swedish Meteorological and Hydrological Institute

[2]Inregia AB

Citation:

Meier, H.E.M., J. Andréasson, B. Broman, L.P. Graham, E. Kjellström, G. Persson, and M. Viehhauser, 2006: Climate change scenario simulations of wind, sea level, and river discharge in the Baltic Sea and Lake Mälaren region – a dynamical downscaling approach from global to local scales. SMHI Reports Meteorology and Climatology No.109, SMHI, SE-601 76 Norrköping, Sweden, 52 pp.

Cover illustration:

The pearl of Lake Mälaren - Stockholm, April 2004. Photo: G. Persson.

RMK
No 109, Feb 2006

Climate change scenario simulations of wind, sea level, and river discharge in the Baltic Sea and Lake Mälaren region – a dynamical downscaling approach from global to local scales

H.E. Markus Meier[1], Johan Andréasson[1], Barry Broman[1], L. Phil Graham[1], Erik Kjellström[1], Gunn Persson[1] and Michael Viehhauser[2]

[1]Swedish Meteorological and Hydrological Institute

[2]Inregia AB

Report Summary / Rapportsammanfattning

Issuing Agency/Utgivare

Swedish Meteorological and Hydrological Institute
S-601 76 NORRKÖPING
Sweden

Report number/Publikation

RMK No. 109

Report date/Utgivningsdatum

February 2006

Author (s)/Författare

Meier, H.E.M., J. Andréasson, B. Broman, L.P. Graham, E. Kjellström, G. Persson, and M. Viehhauser

Title (and Subtitle/Titel

Climate change scenario simulations of wind, sea level, and river discharge in the Baltic Sea and Lake Mälaren region – a dynamical downscaling approach from global to local scales

Abstract/Sammandrag

A regional climate model (RCM) and oceanographic, hydrological and digital elevation models were applied to study the impact of climate change on surface wind, sea level, river discharge, and flood prone areas in the Baltic Sea region. The RCM was driven by two global models and two emission scenarios. According to the four investigated regional scenario simulations, wind speed in winter is projected to increase between 3 and 19% as an area average over the Baltic Sea. Although extremes of the wind speed will increase about as much as the mean wind speed, sea level extremes will increase more than the mean sea level, especially along the eastern Baltic coasts. In these areas projected storm events and global average sea level rise may cause an increased risk for flooding. However, the Swedish east coast will be less affected because mainly the west wind component in winter would increase and because land uplift would compensate for increased sea levels, at least in the northern parts of the Baltic. One of the aims of the downscaling approach was to investigate the future risk of flooding in the Lake Mälaren region including Stockholm city. In Stockholm the 100-year surge is projected to change between -51 and 53 cm relative to present mean sea level suggesting that in the city the risk of flooding from the Baltic Sea is relatively small because the critical height of the jetty walls will not be exceeded. Lake Mälaren lies just to the west of Stockholm and flows directly into the Baltic Sea to the east. This study addresses also the question of how the water level in Lake Mälaren may be affected by climate change by incorporating the following three contributing components into an analysis: 1) projected changes to hydrological inflows to Lake Mälaren, 2) changes to downstream water levels in the Baltic Sea, and 3) changes in outflow regulation from the lake. The first component is analyzed using hydrological modeling. The second and third components employ the use of a lake discharge model. An important conclusion is that projected changes to hydrological inflows show a stronger impact on lake levels than projected changes in water level for the Baltic Sea. Furthermore, an identified need for increased outflow capacity from the lake for the present climate does not diminish with projections of future climate change. The tools developed in this work provide valuable inputs to planning for both present and future operations of water level in Lake Mälaren. Based on the oceanographic and hydrological scenario simulations, flood prone areas were analysed in detail for two municipalities, namely Ekerö and Stockholm. The GIS analysis of both municipalities indicates a series of affected areas. However, in case of the 100-year flood (0.65 m above the mean lake level) in present climate or even in case of the maximum probable flood (1.48 m above the mean lake level) the potential risks will be relatively low.

Key words/sök-, nyckelord

Baltic Sea, Lake Mälaren, scenario simulations, regional climate model, dynamical downscaling, GIS mapping and analysis, flood prone areas, planning

Supplementary notes/Tillägg	Number of pages/Antal sidor	Language/Språk
This work is a part of the EU SEAREG project.	52	English

ISSN and title/ISSN och titel

0347-2116 SMHI Reports Meteorology Climatology

Report available from/Rapporten kan köpas från:

SMHI
S-601 76 NORRKÖPING
Sweden

Contents

1. Introduction

The Baltic is a semi-enclosed sea with a surface area of 386,680 km^2 (without Kattegat). Nine countries share the shorelines of the Baltic Sea and its drainage basin includes territories from 13 countries. Several major cities are located within the basin, with the total population amounting to more than 70 million people. For them, the Baltic Sea is important for economical reasons (shipping, fishery, etc.) and for recreation and leisure activities.

Although the amplitudes of tides are negligible and the risk of coastal flooding is generally smaller than in the North Sea, at some shorelines in the eastern and southern parts storm surges cause problems. For instance, St. Petersburg has been flooded more than 280 times since 1703 (Alenius et al., 1998). The highest measured water level occurred in 1824 and was 4.21 m above mean sea level. In Greifswald the highest water level, since regular measurements have been carried out, occurred on 12-13 November 1872 at 2.77 m above mean sea level (Baerens and Hupfer, 1999). Even higher water levels were reported for February 1625, but documented measurements are not available. Hupfer et al. (2003) summarized observations of other extreme storm surges at the German Baltic Sea coast. Thus, even in the semi-enclosed Baltic Sea storm surges have occasionally severe impact on human life and coastal infrastructure.

In the latest report of the Intergovernmental Panel on Climate Change (IPCC) global sea level rise in simulations with plausible scenarios of greenhouse gas emissions was assessed (Church et al., 2001). As an effect of global warming, thermal expansion and melting glaciers will cause the sea level to increase. The global average sea level is projected to rise between 1990 and 2100 by 0.09 to 0.88 m with a central value of 0.48 m (Church et al., 2001). As a consequence the risk of flooding might increase worldwide.

Regional sea level rise and related issues were addressed within the EU funded project SEAREG (Sea Level Change Affecting the Spatial Development in the Baltic Sea Region). The SEAREG project was performed during the period July 2002 until March 2005 (Schmidt-Thomé, 2006). SEAREG focused on the socio-economic and environmental assessment of climate change in the Baltic Sea region (BSR) specifically for sea level rise and changing runoff patterns of rivers. These can both lead to major flooding events with impacts on cities and regions as well as sustainable development of the entire BSR. One of the case study areas selected within SEAREG was the region surrounding Lake Mälaren, including the Swedish capital Stockholm.

With an average surface area of 1,140 km^2, Lake Mälaren is the third largest lake in Sweden. It lies just to the west of Stockholm and outflows into the Baltic Sea to the east (Fig. 1). The average elevation difference between Lake Mälaren and the Baltic Sea is only 0.66 m. Runoff from a total of 22,600 km^2 drains into the lake. Two of its four outflow points lie to the north and south of the islands of Gamla Stan, which is the old town in central Stockholm. Aside from Stockholm, there are numerous other cities that are situated along its shores. In total, some 2.5 million people live in the vicinity of this lake. For most, Mälaren is also their source of drinking water.

The lake has been regulated by a collection of locks and floodgates since 1943 to maintain a stable water level. This allows for year round navigation on the lake and inhibits saltwater intrusions from the Baltic Sea during periods of high sea level. The regulation also allows for the release of higher outflows than previously possible under natural conditions. The occurrence of water levels reaching the historical highs that took place in the 19th century and early in the 20th century has thus been avoided since regulation began. However, the municipalities along the lake have adjusted to the more stable water levels and modern infrastructure now encroaches into historical floodplain regions along the lakeshore.

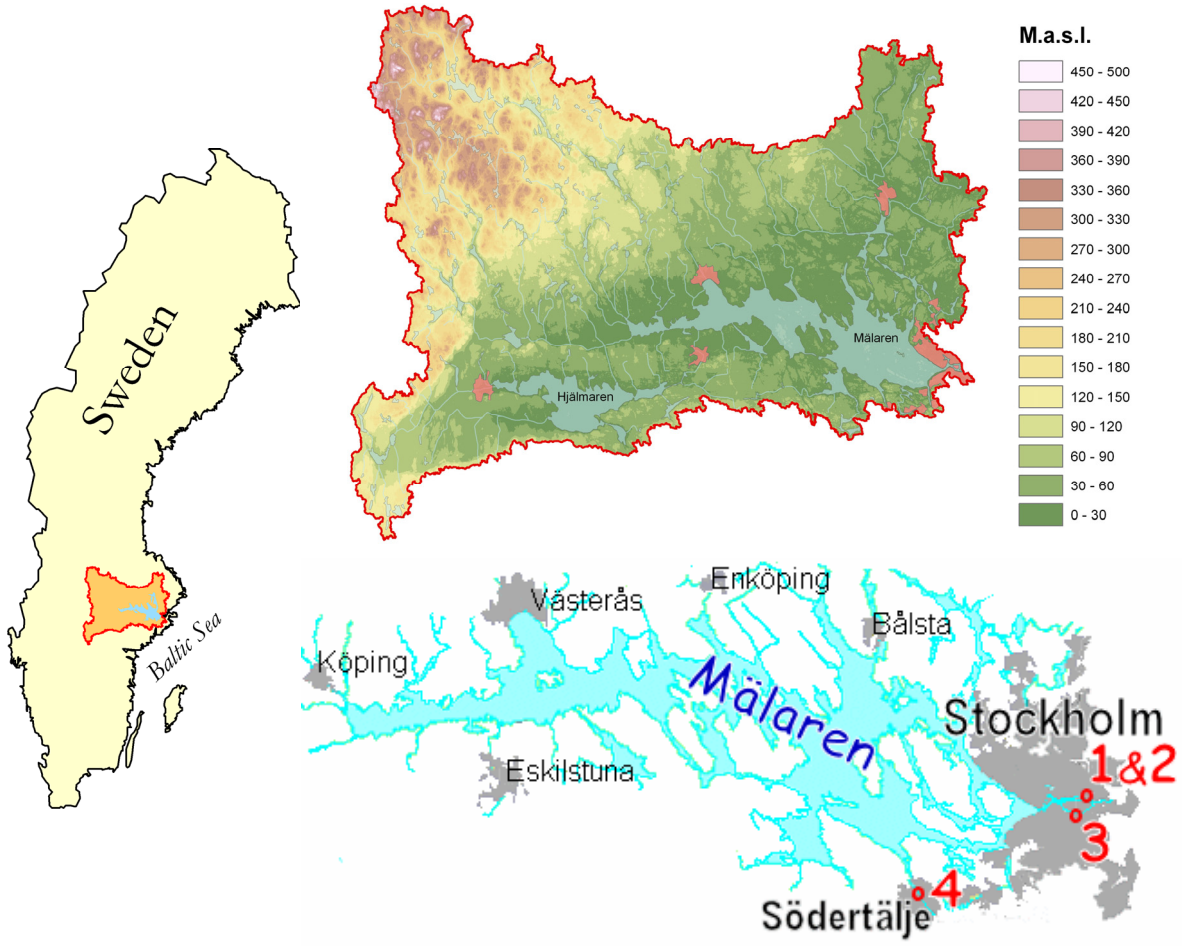

Figure 1. *Location and drainage basin maps for Lake Mälaren. Shown with red numbers are the approximate outflow points from Lake Mälaren to the Baltic Sea at Gamla Stan in central Stockholm (1 and 2), Hammarby (3) and Södertälje (4).*

The water level in Lake Mälaren has in recent years reached high levels that exceeded the guidelines specified in the water court decrees. In the year 2000 the lake level came close to causing major damage to local infrastructure (Fig. 2). Emphasis since then has been put on re-examining both the regulation operating rules for the lake and the hydraulic capacity of the outflow structures. The analysis of this report investigates these issues in

the context of how the water level in Lake Mälaren could be affected by climate change. Three contributing components were looked at in detail: 1) changes to hydrological inflows to Lake Mälaren, 2) effects from changes to downstream water levels in the Baltic Sea, and 3) changes in outflow capacity from Lake Mälaren.

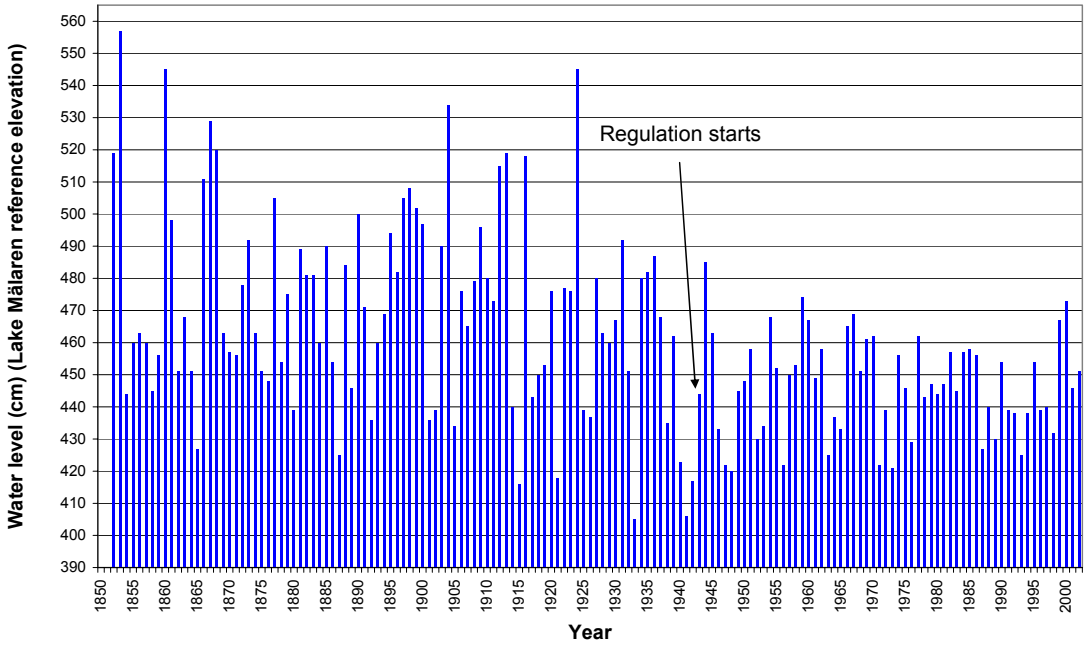

Figure 2. *Maximum yearly water level in Lake Mälaren 1852-2002.*

A downscaling technique was used, which enables the estimation of the possible impact of climate change on water levels in the Baltic Sea and Lake Mälaren region. As the scales of interest are rather small compared to the typical horizontal resolution of global coupled atmosphere-ocean general circulation models (GCMs), a hierarchy of regional models for the wind, sea level, and river discharge was used to break the global signal down to local scales. This technique is called dynamical downscaling.

The report is organized as follows. Section 2 presents the methods utilized. Surface wind in the Baltic Sea catchment area is calculated with a regional climate model (RCM) (section 2.1). The water level in the Baltic Sea is investigated using an ocean circulation model (section 2.2). The water level in Lake Mälaren is calculated using a lake discharge model for the outflow from the lake and hydrological modeling for the inflow (section 2.3). The simulated water levels in the Baltic and Lake Mälaren region are combined with gridded topographical data sets, so-called Digital Elevation Models (DEMs) that allow the calculation of flood prone areas (section 2.4). In section 3 the results of the scenario simulations are presented. The investigated variables are wind (section 3.1), water level of the Baltic Sea (section 3.2), river flow into Lake Mälaren (section 3.3), water level of Lake Mälaren and discharge from the lake (section 3.4), and flood prone areas (section 3.5). In section 3.5 the analysis focuses on two municipalities in the Lake Mälaren region, i.e. Ekerö and Stockholm. In section 4 the dissemination of the modeling results to

concerned regional and local stakeholders are described. The report ends with a discussion (section 5) and conclusions (section 6). The applied model hierarchy of this report is illustrated in Figure 3. For a list of abbreviations the reader is referred to the appendix.

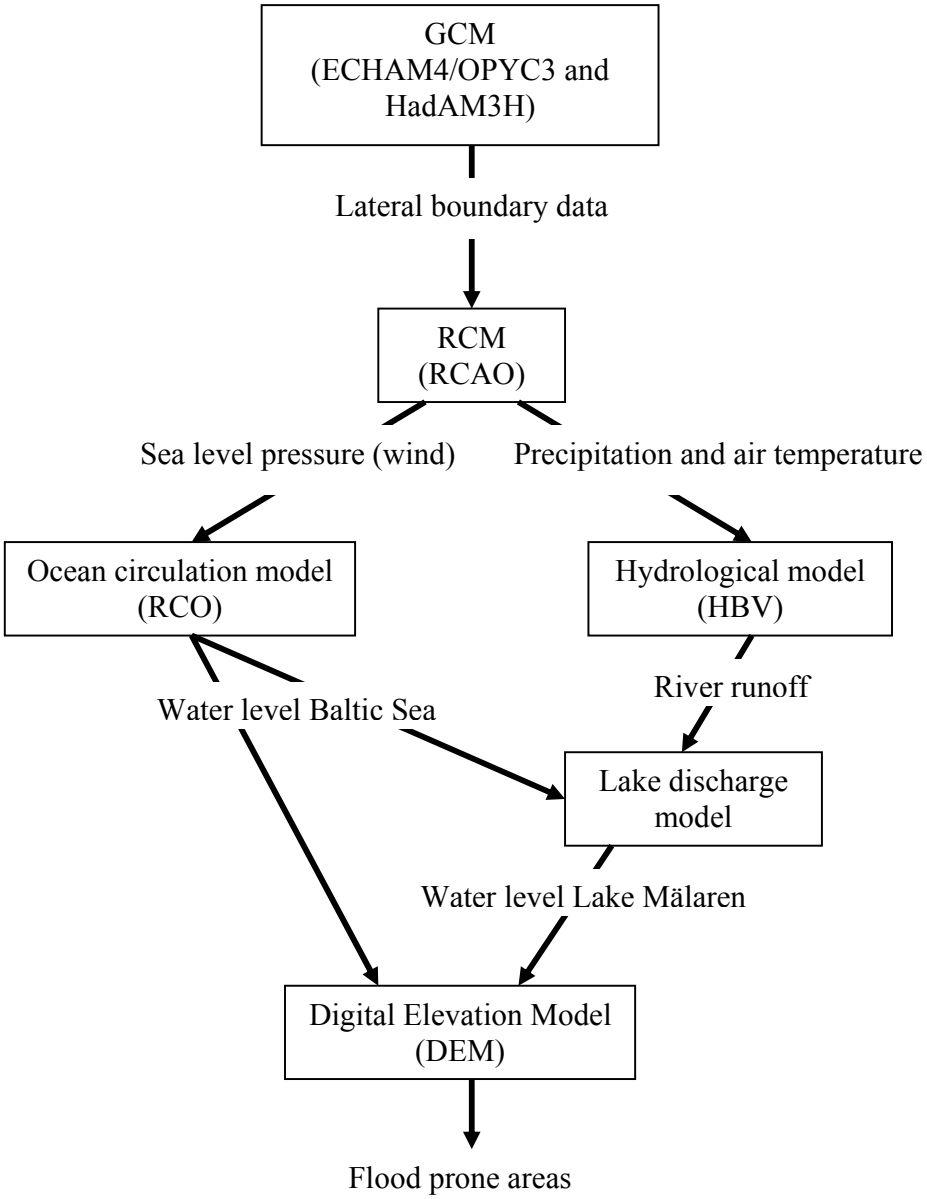

Figure 3. *Scenario simulations of two GCMs (ECHAM4/OPYC3 and HadAM3H) were downscaled utilizing a RCM (RCAO). The results of the RCM were used to force a hydrological model (HBV) and an ocean circulation model (RCO). With these models river flow into Lake Mälaren and water levels in the Baltic Sea were calculated. A lake discharge model provided the water level in the lake and the lake discharge. The impacts of projected changes of water levels in Lake Mälaren and in the Baltic Sea were assessed using gridded topographical data sets, so-called Digital Elevation Models (DEMs). With the depicted hierarchy of models flood prone areas were calculated.*

2. Methods

2.1 Regional climate modeling

The Rossby Centre regional climate model system RCAO (Döscher et al., 2002) is used to calculate climate change scenarios based on two different greenhouse gas emission scenarios (SRES A2 and B2; Nakićenović et al., 2000). Here, RCAO is driven by two different global models, the ECHAM4/OPYC3 model from the Max Planck Institute for Meteorology in Germany (Roeckner et al., 1999) and the HadAM3H from the Hadley Centre in the UK (Pope et al., 2000; Gordon et al., 2000; Jones et al., 2006). Typically the horizontal resolution of GCMs amounts to some 100 km. For the driving GCMs in this study, the horizontal resolution was approximately 150 km for HadAM3H and approximately 250 km for ECHAM4/OPYC3. The horizontal resolution of RCAO was 49 km.

Altogether six different simulations have been undertaken, i.e. one control run (covering the time period 1961-1990) and two scenario runs (2071-2100) with each of the two driving global models. In the following, the control runs will be referred to as RCAO-E and RCAO-H. The corresponding scenario runs have the extension A2 and B2. For a detailed description of these simulations and their results the reader is referred to Räisänen et al. (2003, 2004), Döscher and Meier (2004), Graham (2004), Kjellström (2004), and Meier et al. (2004a, 2004b). RCAO consists of an atmospheric part (RCA2 = RCA version 2) (Jones et al., 2004) and a coupled sea-ice - ocean part (RCO) (Meier et al., 2003).

One source of error in the control experiments is that the boundary data from the GCMs are not without biases. In order to distinguish between errors generated by the RCM and errors imported from the boundaries we make use of `reanalysis´ data as boundary conditions to the RCM. These data sets consist of results from numerical weather prediction models that are driven (and constrained) by as many actual observations as possible to produce representation of critical meteorological variables on a uniform model grid at sub-daily time scales (e.g. ERA15, see Gibson et al., 1997; ERA40, see Uppala et al., 2005). Good agreement between observed and simulated sea level pressure (SLP) in RCA2 forced by reanalysis data has been demonstrated by Jones et al. (2004). In some of the subsequent analyses we use an experiment with RCA2 forced by ERA15-data (Gibson et al., 1997) to evaluate model behavior. This experiment will be denoted with RCA2-ERA15. An overview on data sets used in this report is given in Table 1.

2.2 Sea level simulations

Sea levels were calculated with the Rossby Centre coupled ice-ocean model (RCO) (Meier et al. 2003). In this case, the control run is a hindcast simulation for 1903-1998 utilizing reconstructed atmospheric forcing, observed river runoff, and observed sea level in the northern Kattegat at the open boundary of the model domain (Kauker and Meier, 2003; Meier and Kauker, 2003). In this experiment the wind speed at 10 m height was calculated from reconstructed SLP using a simple boundary layer parameterization over

sea taking the distance to the coast into account (Meier et al., 2003). Hereafter, the reference experiment is denoted with RCO-REF (Tab.1).

In the scenario simulations climatological monthly mean changes of the atmospheric and hydrological forcing were added to the forcing fields of 1903-1998. Such an approach, the so-called *delta change* technique, is frequently applied in hydrological climate change impact studies (cf. section 2.3.2). In this study climatological monthly mean changes were calculated from a series of dynamical downscaling experiments utilizing RCAO. Thus, a series of five 96-year long time slice experiments was performed, i.e. one hindcast simulation for 1903-1998 (RCO-REF) and four scenario simulations of future climate representing 2071-2100. Hereafter, the scenario simulations driven by HadAM3H and ECHAM4/OPYC3 are denoted with RCO-H/A2 or RCO-H/B2 and with RCO-E/A2 or RCO-E/B2, respectively (Tab.1).

Table 1. *Observed and simulated data sets*.

Data set	Variables analysed or used in this report	Time period	Reference
Climatologies and observations			
CRU TS 1.0	Wind speed	1961-1990	New et al. (2000)
SYNOP stations	Wind speed	1/1 1996 – 30/9 2001	SMHI
Tide gauge stations	Sea level	20th century	SMHI
Reanalysis			
ERA40	Wind speed	1961-1990	Uppala et al. (2005)
Simulations			
RCA2-ERA15	Wind speed	1/1 1996 – 30/9 2001	Jones et al. (2004)
RCAO-H	Wind speed	1961-1990	Räisänen et al. (2003)
RCAO-H/B2	Wind speed	2071-2100	Räisänen et al. (2004)
RCAO-H/A2	Wind speed	2071-2100	Räisänen et al. (2004)
RCAO-E	Wind speed	1961-1990	Räisänen et al. (2003)
RCAO-E/B2	Wind speed	2071-2100	Räisänen et al. (2004)
RCAO-E/A2	Wind speed	2071-2100	Räisänen et al. (2004)
RCO-REF	Sea level	1903-1998	Meier (2006)
RCO-H/B2	Sea level	2071-2100	Meier (2006)
RCO-H/A2	Sea level	2071-2100	Meier (2006)
RCO-E/B2	Sea level	2071-2100	Meier (2006)
RCO-E/A2	Sea level	2071-2100	Meier (2006)

The use of RCO-REF as control simulation has the advantage that sea level extremes are simulated in good agreement to observations (Meier, 2006) whereas in the control simulations of the coupled atmosphere-ice-ocean model, RCAO-H and RCAO-E, simulated sea level extremes are considerably underestimated due to underestimated wind speed extremes (see section 3.1). In addition, the uncertainty of the simulated changes in the RCO experiments due to natural variability is reduced compared to the RCAO results because the simulations are more than three times longer.

To estimate the impact of the uncertainties of the global and regional model results and the emission scenarios of anthropogenic greenhouse gases, we calculated three sea level projections. First, a `high case´ projection was estimated using the regional model results with the largest sea level changes (RCO-E/A2) together with the upper limit for the projected global average sea level rise of 0.88 m (Church et al., 2001). However, one should keep in mind that on the regional scale horizontal patterns of the projected sea level rise in the global scenario simulations can differ significantly (Church et al. 2001, Fig. 11.13). Therefore, our `high case´ projection might be lower than what would be the absolute worst case based on global climate change scenario simulations. Second, an `ensemble average´ was calculated from the four regional scenario simulations (RCO-H/B2, RCO-H/A2, RCO-E/B2, and RCO-E/A2), assuming a global average sea level rise of 0.48 m, which is the central value for all scenario simulations presented by Church et al. (2001). Third, a `low case´ projection was estimated using the regional model with the smallest sea level changes (RCO-H/B2) together with the lower limit for the global average sea level rise of 0.09 m. In all three projections (`low case´, `ensemble average´, `high case´) land uplift was considered. Absolute land uplift rates were calculated from land uplift relative to the mean sea level according to Ekman (1996) adding a past eustatic sea level rise of 1.5 mm yr^{-1} (Church et al., 2001).

Sea level extremes were analyzed in terms of 100-year surges, i.e. Gumbel distributions were fitted to each series containing 96 annual maximum sea level values to provide estimates of the surge height at the return period of 100 years. The statistical significance of the changes was estimated using a bootstrap with resampling of the original annual maximum sea level data (Wilks, 1995). The bootstrap operates by constructing 1000 artificial data batches using sampling with replacement from the original data. Thus, the statistics of 1000 artificially generated 100-year surges in present and future climates were compared. Assuming normally distributed 100-year surge heights the standard Student's *t*-test was applied to decide whether changes of the sea level extremes are statistically significant or not. Alternatively, the change is considered to be statistically significant if the number of cases in which the resampled scenario return value is larger than the resampled control return value is larger than 99% of all cases.

Another significance test is the pool permutation procedure (Jouni Räisänen, University of Helsinki, pers. comm.). The two time series of the 96-year control and 96-year scenario simulations were concatenated to a single 192-year time series. At random 96 yearly values for `sample 1´ were selected. `Sample 2´ consisted of the remaining values. For both samples the 100-year return values and their difference were calculated. This procedure was repeated 1000 times. If the number of cases in which the difference

between the `sample 2´ and `sample 1´ return values is larger in absolute values than the difference between the true scenario and control samples is smaller than 1%, the difference between the 100-year surges of the control and scenario simulations is regared as statistically significant.

The model results were analyzed based upon 6-hourly snapshots. As a reference system the Nordic Height system 1960 (NH60) is used (Ekman and Mäkinen, 1996).

2.3 Water level simulations for Lake Mälaren

The first step of the investigation to calculate water level in Lake Mälaren used hydrological modeling to analyze changes to runoff inflow to Lake Mälaren due to climate change. The modified inflows were then input into a lake discharge model that simulates in detail the outflow from the lake including the regulation to maintain stipulated water levels. The lake discharge model was used to carry out the second and third steps of the analysis, which looked at how climate change could affect operation of the hydraulic structures and resulting lake levels. Although the question of maintaining a minimum water level in Lake Mälaren is also important for future management, this study focused primarily on high water levels and the potential for flooding.

According to the RCO `high case´ scenario simulation, the projected winter mean sea level rise at Stockholm for the future period of 2071-2100 was estimated to 0.46 m (Meier et al., 2004a; Fig. 7). Although sea levels can vary considerably during short periods of time, this value was used here in the lake discharge analyses to test the sensitivity of Lake Mälaren regulations to changes in sea level.

2.3.1 Hydrological modeling

Projecting hydrological change from the climate scenarios was performed using a hydrological model, the HBV model (Bergström, 1995; Lindström et al., 1997). This conceptual semi-distributed runoff model was originally developed for operational runoff forecasting. It has also been used extensively in impact assessment studies, both for climate change (Andréasson et al., 2004; Bergström et al., 2001; Gardelin et al., 2002; Vehviläinen and Huttunen, 1997) and for water quality (Arheimer and Brandt, 1998), and even for combinations of the two (Arheimer et al., 2005). The model is usually run on a daily timestep and includes routines for snow accumulation and melt, soil moisture accounting, groundwater response and river routing. Input data to the model are precipitation, temperature and potential evapotranspiration estimated with a temperature index method (Lindström et al., 1997).

The HBV model is typically calibrated against river flow observations with the help of an automatic calibration routine (Lindström, 1997) to obtain optimal performance in terms of a combination of seasonal dynamics and water volume balance. For lakes, one often uses observed outflow observations from the lake for calibration. For Lake Mälaren, however, as the lake is strongly regulated and as the primary focus was to examine changes in lake water level, it was important to obtain good model representation of the

inflows to the lake. Thus, the calibration was performed against total inflow to the lake for the period 1963 to 1990.

Obtaining total inflow to Lake Mälaren is not a straightforward process as flows from all tributary rivers and streams are not routinely measured. Therefore, a synthetic inflow series was created from observed changes in lake water level combined with observed (regulated) lake outflow. As the lake is so large, a complicating factor is that even small changes in water level lead to large changes in volume. For example, a change of only 1 cm per day corresponds to an inflow of 11 million m^3 per day, or about 130 m^3s^{-1}. Small deviations in measurement of water level, which can be caused by waves or tilting of the lake surface due to prevailing winds, can therefore create large errors in calculated change in volume. Due to this, it was necessary to apply a filter to measured water levels before using them to calculate inflow. This was the Savitzky-Golay smoothing filter (also called digital smoothing polynomial filters or least-squares smoothing filters, see Press et al., 1999), which was applied with a nine day time frame.

The hydrological calibration resulted in an efficiency criterion, R^2 (Nash and Sutcliffe, 1970), of 0.70 and a relative volume error of 0.1%. Using this efficiency criterion, a perfect fit would be 1.0 and typical values for well-calibrated basins often lie between 0.8 and 0.95. Nevertheless, taking into account the uncertainties in the observations used, the Lake Mälaren calibration was deemed reasonably representative. The efficiency criterion, as applied here, is weighted more toward representing high inflows of short duration. For Mälaren, it was particularly important that the inflow volume error was low as this is more critical for determining water level in large lakes.

2.3.2 Linking hydrology to climate scenario simulations

Transferring the signal of climate change from climate models to hydrological models requires an interface. Although the performance of climate models has improved considerably in recent years, systematic biases still persist in precipitation, the most important climatological variable for hydrological applications. Biases occur not only with precipitation amounts but also with its seasonal representation. Therefore, the hydrological impact studies were done with offline simulations from the HBV model, using an observed database as a reference climate. Changes in meteorological variables, i.e. precipitation, temperature and evapotranspiration, between the control and the scenario simulations from the RCAO regional climate model were processed in a model interface before being transferred to the observed climate database, as depicted in Figure 4. This can be referred to as the *delta change* approach (cf. section 2.2) and is a common method of transferring the signal of climate change from climate models to hydrological models (Arnell, 1998; Bergström et al., 2003; Gellens and Roulin, 1998; Graham, 2004; Middelkoop et al., 2001).

RCAO climate model outputs were first spatially averaged over the Lake Mälaren drainage basin before transfer via the interface to the hydrological model. For precipitation, the monthly average relative change was smoothed to a 3-month-running-mean and then applied to each daily observation. The same monthly change factors were

used for all years of the impact simulations, for extreme values as well as for average conditions. As a relative change was applied to an observed database, the method does not alter the number of days with precipitation in the scenario climate. A drawback of this procedure is that information about changes in climate variability is lost in the process.

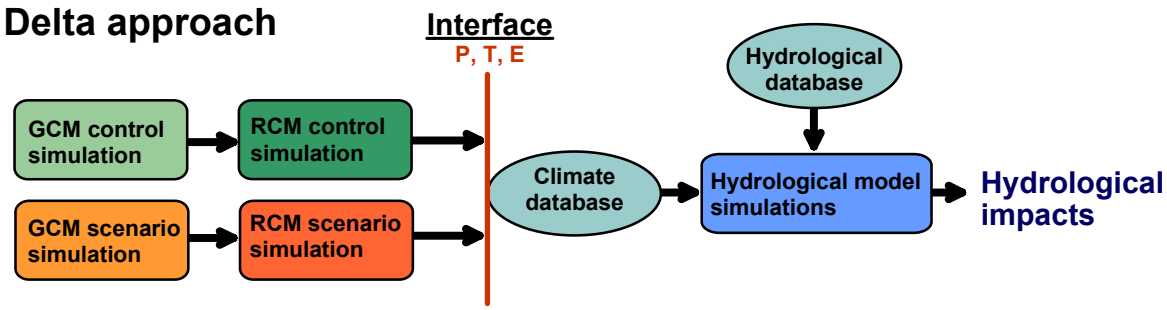

Figure 4. *The analysis chain for assessments of hydrological impacts from climate change simulations (P = precipitation, T = temperature, E = evapotranspiration).*

The temperature change was transferred using a set of seasonal linear transfer functions in which the magnitude of the temperature change varies according to the daily temperature in the reference climate. This accounts for the fact that the change in winter temperature in the scenario simulations is strongest at low temperatures and less pronounced at higher temperatures (Andréasson et al., 2004). However, in summer changes of the high temperatures are larger than changes of the low temperatures except in the northernmost part of the Baltic catchment area (Kjellström, 2004).

Changes in evapotranspiration can be as important as changes in precipitation for the outcome of hydrological impact simulations. Evapotranspiration was calculated using a temperature-index method. To preserve consistency between the climate model simulations and the HBV simulations, the actual evapotranspiration calculated from the HBV model was adjusted so that it results in the same yearly increase as given by the respective climate model simulations.

2.3.3 Lake discharge modeling

Due to the number of structures involved and the regulation specifications outlined by the Swedish Lake Water Court, it is not a simple matter to calculate the discharge from the lake at a given point in time. A model was therefore set up that simulates the different physical and legal conditions required in regulating the water level of the lake. This incorporates the specific hydraulic equations of all of the hydraulic structures together with appropriate timing of releases as dictated by water level according to the Water Court Decree.

Lake Mälaren has its own elevation reference system that is based on the threshold of Karl Johan Lock located between Gamla Stan and the Stockholm neighborhood referred to as Slussen. This is the defined `zero´ point for this system, which corresponds to an elevation of -3.48 m in the RH70 elevation reference system. Water levels for Lake

Mälaren are typically expressed in centimeters, so that the mean water level 1961-1990 for the lake is 415 cm in the Mälaren reference system (i.e. +0.67 m in the RH70 height system). All results from the lake discharge modeling are given in the Mälaren reference system.

Regulation of the water level in the lake is dictated by decrees handed down by the Swedish Water Court. The original decree was established in 1941. This was followed by an additional decree in 1966 (Ehlert, 1970), which was in turn slightly modified in 1989. The water decrees are official documents that stipulate in detail the relative lake levels for either releasing or storing water in Lake Mälaren. Henceforth, these operating rules will be referred to collectively as the Water Court Decree. The aim of the water court was threefold: 1) to maintain a minimum water level for navigation between the Baltic Sea and Lake Mälaren communities, 2) to allow for the controlled release of water to avoid the occurrence of high lake water level resulting in flood conditions, and 3) to prohibit the inflow of saltwater from the Baltic during periods of high sea level to preserve quality in the municipal water supply.

The Water Court Decree specifies that under normal conditions Lake Mälaren should be regulated such that the water level is maintained at a desired target of 415 cm, and for conditions with high inflows should not be allowed to exceed 470 cm in the Mälaren reference system. Navigation locks and floodgates control the outflow of water from Lake Mälaren at four different locations as mentioned in the introduction (section 1). These are shown as four points on the map in Figure 1. In total, there are eight different hydraulic structures that are used in combination to regulate lake levels, as listed in Table 2. As four of these are locks used for navigation, the Ports of Stockholm is the agency in charge of coordinating all of Lake Mälaren's regulation structures.

Table 2. *Locks, floodgates and estimated outflow capacity under normal operating conditions for the regulation of Lake Mälaren. The numbers under location correspond to the numbers shown on the map in Figure 1.*

Location (no. on map)	Name	Approximate Capacity (m^3s^{-1})
Norrström (1) (north of Gamla Stan)	Riksbron	200
	Stallbron	100
Slussen (2) (south of Gamla Stan)	Karl Johan Discharge Canal	120
	Karl Johan Lock	140
Hammarby (3)	Skanstull Culvert	5
	Hammarby Lock	70
Södertälje (4)	Maren Culvert	5
	Södertälje Lock	70
	Total	710

The combined outflow capacity from these hydraulic structures is currently estimated at 710 m^3s^{-1} for average water levels. However, this capacity varies according to the water levels in both Lake Mälaren and downstream in the Baltic Sea. At a water level of 470 cm (target maximum), this can reach more than 840 m^3s^{-1} for a low water level in the Baltic. At a high water level in the Baltic, this can be less than 710 m^3s^{-1}. If lake water levels exceed the desired maximum of 470 cm, outflow capacity can also reach higher values.

An important stipulation of the Water Court Decree is that outflow through each of the locks at both Hammarby and Södertälje should not be greater than 70 m^3s^{-1}. Although it is physically possible to exceed this flow, doing so results in excess velocities in the downstream channels that can cause erosion to occur and lead to safety problems. This has happened on occasion, but only under emergency conditions; it should be avoided whenever possible.

2.4 Spatial modeling

A regional Digital Elevation Model (DEM) within a Geographical Information System (GIS) at a scale 1:50,000 was used for a rough assessment of water level impacts in the Lake Mälaren region. The vertical accuracy of the model was only 0.5 m and the horizontal grid lengths were about 50 to 100 m. The regional assessment results were therefore uncertain and only usable for general reflections. However, they helped to identify potential risk areas, which were the basis for two selected local DEM assessments in Ekerö and Stockholm. The approach provided identification of `hot spots´.

Better quality elevation data were obtained for these two municipalities (accuracy varies between 2 and 25 cm vertical resolution) and allow detailed studies of flood risk areas. The identified flooding areas were matched with relevant spatial data such as population, working places, infrastructure, housing estates, industrial sites, waste deposits and other spatial facilities. Those data sets were then transformed to local risk zone maps of potential flood prone areas. This work opens up possibilities for diverse applications in local spatial planning, as listed below:

- basic data for municipal risk and vulnerability assessment,
- guidance information for general land use planning (e.g. comprehensive plans),
- input to overall planning of various urban service works,
- platform for detailed surveys to identify and perform permanent risk prevention measures.

Coarse scale overview maps of floodplain extent were previously created by SMHI for the Swedish Rescue Services (SRV, 2001) to be used for preparedness planning within present climate. These maps are based on hypothetical extreme inflows to Lake Mälaren that were calculated to represent both the 100-year design flood and the estimated maximum probable flood (MPF). Results from the previous work showed that water levels in Lake Mälaren's reference system resulting from these two design floods would reach 480 cm (65 cm above mean sea level) and 563 cm (148 cm above mean sea level),

respectively. These two levels were used for comparison to the lake discharge results (section 3.4). They were also used in the flooding sensitivity studies using GIS analysis (section 3.5).

3. Results

3.1 Wind speed

In the present section the wind climate in the RCAO model is analyzed. First we assess the model performance for the control period (1961-1990). The simulated mean wind is compared with gridded climatologies and reanalysis data. In addition, we compare observational data for open sea and coastal SYNOP stations in the Baltic Sea area. The observational records at these stations are compared to the model output not just for mean wind but also for the probability distribution of daily wind speed.

When the ability of RCAO to simulate the wind climate is assessed for the control period we analyze four climate change scenario simulations for a changing wind climate. Here changes in both wind speed and direction are discussed. Also changes in probability distributions of daily wind speed are investigated.

3.1.1 Model performance in present climate (1961-1990)

The wind climates in the control simulations and the climate change scenario simulations used in this study have previously been analysed and discussed in Räisänen et al. (2003), Pryor and Barthelmie (2004), and Pryor et al. (2005). For the two control simulations (RCAO-E and RCAO-H) Räisänen et al. (2003) showed that biases in the simulated wind speed are related to biases in SLP. However, both simulated annual mean wind speed and seasonal cycle are in relatively good agreement with the observational data from the Climate Research Unit (CRU, see New et al. 1999; 2000) in the Baltic Sea runoff area. Also compared to the reanalysis data from the National Centers for Environmental Protection, NCEP (Kalnay et al., 1996; Kistler et al., 2001), a high degree of correspondence in terms of the magnitude and spatial patterns of the flow characteristics was shown for the two control simulations by Pryor and Barthelmie (2004) and Pryor et al. (2005).

Here we look further into the simulated seasonally averaged wind speed as compared to CRU and also to the ERA40 reanalysis data set (Uppala et al., 2005), see Figure 5. Notably the ERA40-data show very low wind speed over the mountainous terrain in Scandinavia compared both to CRU and especially to RCAO. The reason for the low wind speed in ERA40 in these regions is the large surface roughness used in the ECMWF model (Per Kållberg, SMHI, pers. comm.). In other parts of the region there are many similarities between RCAO and ERA40 such as land-sea contrasts in coastal and low altitude land areas as well as the absolute numbers over the Baltic Sea during all seasons.

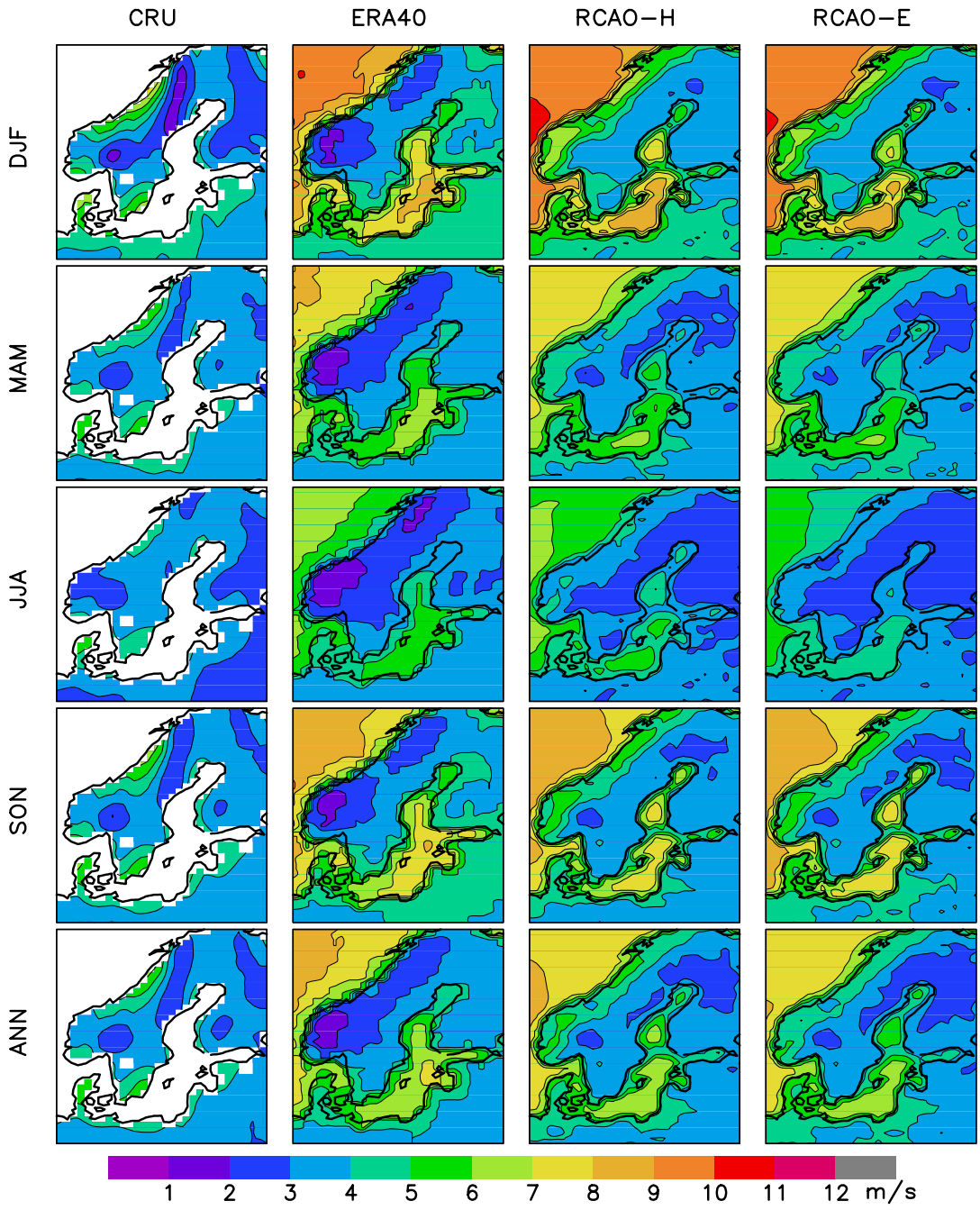

Figure 5. *Seasonal average wind speed. To the left are data on a 0.5°x 0.5° (roughly 55 km x 55 km) grid from the Climate Research Unit (CRU, see New et al., 2000), the second column shows data on a 125 km x 125 km grid from the ERA40 data set (Uppala et al., 2005) while the two columns to the right show the RCAO control climate on a 0.44° x 0.44° (50 km x 50 km) grid. All data sets represent the time period 1961-1990.*

Still some differences over the Baltic Sea can be noted. During winter the wind speed in the southern parts of the Baltic proper is stronger in RCA than in ERA40, during the

other seasons (especially fall) ERA40-wind speeds are stronger in the Baltic proper, the Bothnian Sea and in the Gulf of Finland. These differences may be related to the above mentioned errors in SLP. In winter the north-south pressure gradient over much of Europe is too strong in the control simulations presumably leading to the too strong winds (Räisänen et al., 2003; Fig. 3). In spring and fall slightly too weak north-south pressure gradients are simulated leading to the low wind speeds.

Comparing RCAO with CRU reveals some differences, particularly during winter. The winter time differences over Sweden between RCAO and CRU were discussed by Räisänen et al. (2003). Räisänen et al. (2003) suggested some problem in the simulation of boundary layer stability conditions or stability dependence of the near-surface wind speed. They also mentioned the fact that the stations used in the CRU data set are to a large extent situated in low-lying (valley) stations in northern Sweden making them less windy than surrounding higher terrain. From Figure 5 it can be noted that the seasonality of wind speed in parts of northern Scandinavia is reversed in CRU as compared to RCAO. Although the ERA40 wind speeds are biased, as discussed above, it could be noted that the seasonal cycle of wind speed over inland areas in Scandinavia is similar in ERA40 to RCAO. This similarity indicates that the representativity of valley stations is indeed a problem when CRU data are compared to model results.

The geographical patterns in RCAO-H and RCAO-E are very similar to each other in all seasons. Also the absolute numbers are more or less the same in all seasons except in summer when RCAO-E shows slightly lower wind speeds over most of the area north of the Danish, German, and Polish coasts in accordance with a slightly weaker pressure gradient in this area (Räisänen et al., 2003; Fig. 3). It could also be noted that the wind speed in summer is lower in RCAO as compared to both ERA40 and CRU over near-coast areas in northern Sweden and Finland.

We compared the simulated (RCA2-ERA15) and observed wind speed at 23 SYNOP stations surrounding the Baltic Sea (Tab. 3). From the model we extracted wind information from the gridbox closest to the observational location. The comparison was made for the time period 1 January 1996 to 30 September 2001 with a time interval of 3 hours. In general the model underestimates the wind speed both in terms of mean and median values with 1-2 m/s although there are exceptions with overestimations at some locations. Notably, for all the stations along the Baltic coast (Liepaja, Hel, Ristna and Klapeja) the wind speed is overestimated. Figure 5 indicates stronger wind speed in the ERA40 data than what is observed according to CRU east of the Baltic Sea. It may therefore be that the boundary data from ERA15 (that are similar to those in ERA40) lead to higher wind speed in this area as compared to the gridded climatology.

Table 3. *Comparison between model (RCA2-ERA15) and SYNOP observations every 3rd hour during the time period 1 January 1996 to 30 September 2001. The categorical statistics for exceeding two thresholds are shown as probability of detection (POD), false alarm ratio (FAR) and true skill score (TSS), see text for definitions. Stations marked with yellow are those where the land cover in the corresponding model grid point is at most 25%. See next page.*

Synop station	Lat	Long	Model grid		Model bias and errors (monthly means)					Categorical statistics exceeding 8 m/s			exceeding 12 m/s		
			land fraction	orogra-phy (m)	mean (m/s)	mean (%)	p99 (m/s)	p99 (%)	Corre-lation	POD	FAR	TSS	POD	FAR	TSS
Liepaja	56° 28'	21° 1'	0,15	6,2	1,9	54,5	2,3	21,7	0,8	0,66	0,16	0,50	0,32	0,01	0,31
Hel	54° 36'	18° 49'	0,33	57,6	1,2	29,5	2,0	19,0	0,8	0,56	0,12	0,44	0,19	0,01	0,18
Ristna	58° 55'	22° 4'	0,16	2,6	1,0	23,6	-0,2	-6,1	0,8	0,33	0,09	0,23	0,03	0,00	0,02
Gotska Sandön	58° 23'	19° 11'	0,00	0,1	1,0	18,1	1,6	11,3	0,8	0,59	0,24	0,36	0,53	0,06	0,47
Klapeja	55° 43'	21° 4'	0,38	20,5	0,3	3,5	-0,4	-7,7	0,8	0,45	0,08	0,37	0,16	0,00	0,16
Russarö	59° 46'	22° 56'	0,04	1,7	-0,2	-3,4	-1,2	-10,3	0,9	0,42	0,12	0,30	0,20	0,01	0,19
Holmögadd	63° 35'	20° 45'	0,01	4,2	-0,5	-9,9	-1,5	-13,5	0,8	0,36	0,07	0,29	0,07	0,00	0,06
Ölands norra udde	57° 22'	17° 5'	0,05	3,4	-0,8	-13,1	-2,3	-18,6	0,8	0,32	0,08	0,24	0,08	0,00	0,08
Landsort	58° 44'	17° 52'	0,02	3,0	-1,0	-14,3	-2,2	-16,0	0,8	0,42	0,11	0,30	0,11	0,01	0,10
Svenska Högarna	59° 26'	19° 30'	0,00	0,1	-1,1	-14,5	-2,7	-17,9	0,9	0,50	0,15	0,35	0,16	0,01	0,15
Hammerodde	55° 17'	14° 46'	0,13	14,0	-1,4	-20,3	-4,3	-25,8	0,8	0,41	0,12	0,29	0,12	0,01	0,11
Falsterbo	55° 23'	12° 49'	0,52	18,9	-1,2	-20,3	-3,6	-25,8	0,7	0,30	0,05	0,25	0,06	0,00	0,06
Fårösund	57° 55'	18° 57'	0,28	6,6	-1,3	-21,4	-3,9	-29,7	0,8	0,26	0,05	0,21	0,01	0,00	0,01
Arkona	54° 40'	13° 25'	0,18	3,4	-1,6	-21,5	-4,1	-25,6	0,8	0,42	0,09	0,33	0,11	0,01	0,11
Utö	59° 46'	21° 22'	0,04	1,7	-1,7	-25,2	-3,9	-26,2	0,9	0,31	0,08	0,24	0,07	0,00	0,07
Brämön	62° 13'	17° 44'	0,19	33,1	-1,8	-31,2	-5,6	-40,1	0,7	0,10	0,02	0,09	0,00	0,00	0,00
Skags_udde	63° 11'	19° 1'	0,54	62,5	-1,6	-32,7	-5,1	-41,7	0,7	0,03	0,00	0,03	0,00	0,00	0,00
Rödkallen	65° 18'	22° 22'	0,14	14,0	-1,9	-33,6	-4,3	-34,2	0,7	0,09	0,01	0,08	0,00	0,00	0,00
Nidingen	57° 18'	11° 54'	0,46	25,8	-2,7	-38,4	-5,9	-38,6	0,8	0,16	0,01	0,14	0,01	0,00	0,01
Måseskär	58° 5'	11° 19'	0,39	23,4	-2,8	-39,0	-6,1	-38,7	0,9	0,17	0,02	0,16	0,01	0,00	0,01
Bjuröklubb	64° 28'	21° 34'	0,39	23,8	-2,6	-42,0	-6,8	-47,2	0,8	0,05	0,00	0,04	0,00	0,00	0,00
Lungö	62° 38'	18° 5'	0,79	131,8	-2,6	-44,0	-7,9	-53,9	0,7	0,02	0,00	0,02	0,00	0,00	0,00
Örskär	60° 31'	18° 22'	0,61	12,3	-3,7	-50,8	-8,4	-52,7	0,8	0,03	0,01	0,02	0,00	0,00	0,00

Differences between model results and observations can partly be related to the observations. Some measurement sites may be sheltered by obstacles like buildings or vegetation in some wind directions and some may measure wind at other levels than 10 m above the ground. Also, the observational sites are point measurements and may therefore not be representative for larger areas like the 50 km x 50 km gridboxes used in the RCM. In the following we have therefore excluded those stations for which the land fraction of the model grid box exceeds 25% leaving 13 of the 23 stations. For this selection of stations the model underestimates the wind speed at 10 sites while the remaining three are overestimated, the range of biases lies between ±1.9 m/s.

The model fails to produce proper high wind speeds. The underestimation as seen in the mean wind speed grows worse at most stations when the 95th and 99th percentiles are investigated. This underestimation often reaches several m/s indicating a larger problem in simulating high wind speeds although some of the discrepancies may also be related to the quality and representativity of point measurements as outlined above. Problems at higher wind speeds can also be seen in the categorical statistics presented in Table 3. Given a threshold of 8 m/s the probability of detection (POD = the fraction of observed events that were correctly forecasted) ranges from roughly 10 to 67% at the 13 stations. In combination with the false alarm ratio (FAR = the fraction of forecasted events that were observed to be non events) this makes the true skill score (TSS = POD-FAR, ideally it should take the value 1) ranging from between less than 0.1 to at best 0.5 for these stations. Since the model has a problem in simulating higher wind speeds FAR decreases with increasing threshold (cf. Tab. 3). But since also POD decreases TSS decreases rapidly for higher wind speeds.

Landsort is one of the few stations in Table 3 with the most suitable location for representing open sea conditions (Hans Alexandersson, SMHI, pers. comm.). We compared the simulated wind speed in the two control runs to the observed climatology at Landsort for the same time period (1961-1990). In addition, we compared reanalysis-driven runs (boundaries from ERA15, see Gibson et al., 1997) with observations for the time period used in Table 3. The results are summarized in Table 4. It can be seen from Table 4 that the error in mean wind speed is substantially smaller in the reanalysis-driven simulations compared to the control simulations. It is reduced to 67% of the error in RCAO-H and 53% of the error in RCAO-E. For the high wind speeds (99th percentile) the error reduction is similar, i.e. 50-55%. Regardless of this reduction the remaining error of more than 2 m/s for the 99th percentile indicates that the problem of simulating high wind speeds does not lie solely in the boundary conditions. It is a common feature among RCMs to underestimate high wind speeds unless they include a more explicit treatment of gustiness (Rockel, 2004; Rockel and Woth, 2005).

Table 4. *Bias in wind speed at Landsort (58.74°N, 17.87°E). The bias is given for the mean wind speed and for the 99th percentile. Both absolute (m/s) and relative (%) errors are given. For RCAO the comparison is made for the entire period 1961-1990. For RCA2-ERA15, the comparison is made with observations from the period January 1996 to September 2001.*

Experiment		(m/s)	(%)
RCAO-E	Mean	-1.9	-27.2
	99th percentile	-4.9	-28.2
RCAO-H	Mean	-1.5	-20.5
	99th percentile	-4.4	-24.2
RCA2-ERA15	Mean	-1.0	-14.3
	99th percentile	-2.2	-16.0

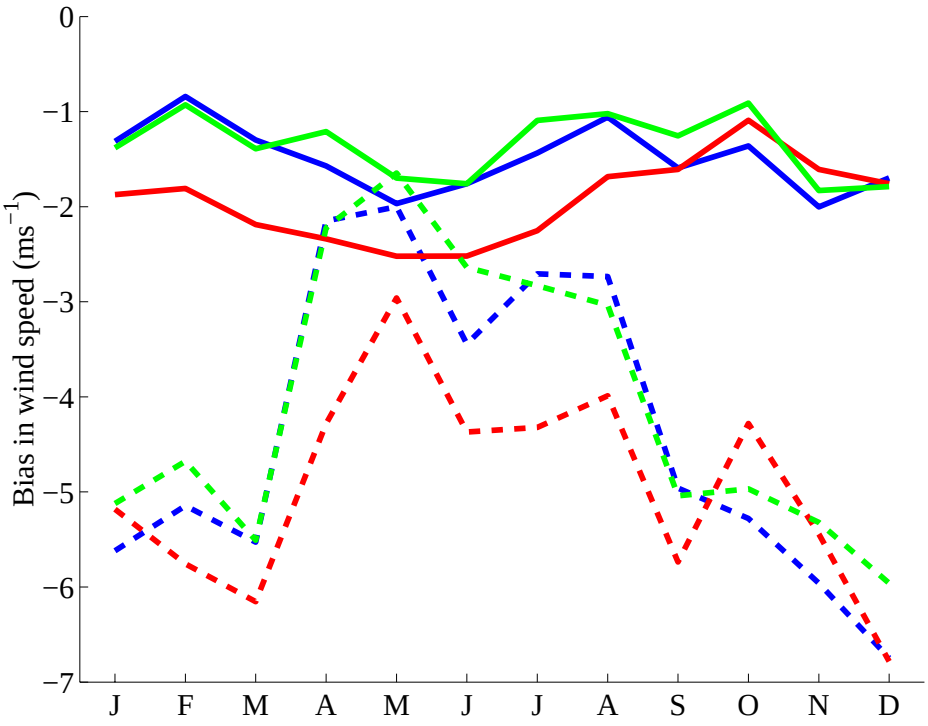

Figure 6. *Seasonal cycle of the bias in mean wind speed (full lines) at Landsort (58.74°N, 17.87°E). Dashed lines show the bias in the 99th percentile of 3-hourly wind speed. Shown is the bias in RCAO-E (red), RCAO-H (blue), and RCA2-ERA15 (green).*

The bias in mean wind speed at Landsort is rather uniform during the year (Fig. 6) showing that the model captures the seasonal cycle. This can be generalized also to the other stations in Table 3 since the correlation coefficients of the monthly mean wind speed are fairly high (more than 0.7) for all stations. At the same time the bias in high

wind speed is much larger during the winter half of the year than during summer. It is during this part of the year when the absolute wind speeds are highest. During the summer half of the year the wind speed is more moderate. For Landsort the biases in the simulation with RCAO-E are larger than in RCAO-H (Fig. 6). This is a large-scale feature in large parts of the model domain (as noted for SLP in Räisänen et al., 2003) probably due to the fact that the HadAM3H-simulation was forced with observed sea surface temperatures while ECHAM4/OPYC3 is a fully coupled AOGCM. Therefore, it has more freedom to develop its own climate.

3.1.2 Scenario simulations

Table 5 shows area averaged seasonal changes in mean wind speed in the scenario runs as compared to the control climate for the Baltic Sea and Kattegat. The RCAO scenario runs driven by ECHAM4/OPYC3 show increases in the wind speed during winter and spring in the range of 10-20%. In the other seasons and also in all seasons in the RCAO scenario runs driven by HadAM3H the differences are about 5% or less.

Table 5. *Area average seasonal changes (%) in mean wind speed over the Baltic Sea and Kattegat (DJF = December, January, February, etc.). Changes that are at the 95% level statistically significant are given in bold.*

	DJF	MAM	JJA	SON
RCAO-E/A2	**18.5**	**14.9**	**-5.9**	**4.2**
RCAO-E/B2	**12.1**	**9.4**	**-4.9**	**3.8**
RCAO-H/A2	**4.5**	1.1	3.3	-3.3
RCAO-H/B2	3.1	-0.7	**5.7**	1.5

The simulated changes were compared to the magnitude of the year-to-year variability in the simulations following the approach as outlined by Räisänen et al. (2003). In this comparison we applied a *t*-test where the error variance of the simulated change is adjusted to take into account positive correlation between subsequent years. In Table 5 it is indicated when the climate change signal is statistically significant. A signal is defined here as statistically significant when the chance of such a signal occuring is less than 5% by pure chance. The changes in RCAO-E/A2 and RCAO-E/B2 are statistically significant in all seasons while the changes in RCAO-H/A2 and RCAO-H/B2 generally are not.

Figure 7 shows the geographical distribution of these changes in the Baltic area. Here the differences between the driving models are emphasized. The RCAO-H runs show much smaller changes during winter and spring than the RCAO-E runs, both over the Baltic Sea and especially over the adjacent land areas. The large differences between the RCAO-E and RCAO-H runs during winter and spring can be attributed to the large differences in the driving global models. In ECHAM4/OPYC3 a stronger pressure gradient between northern and central Europe is simulated in the scenario runs as compared to that simulated in HadAM3H. This difference leads to stronger westerlies in northern Europe as shown by Räisänen et al. (2003).

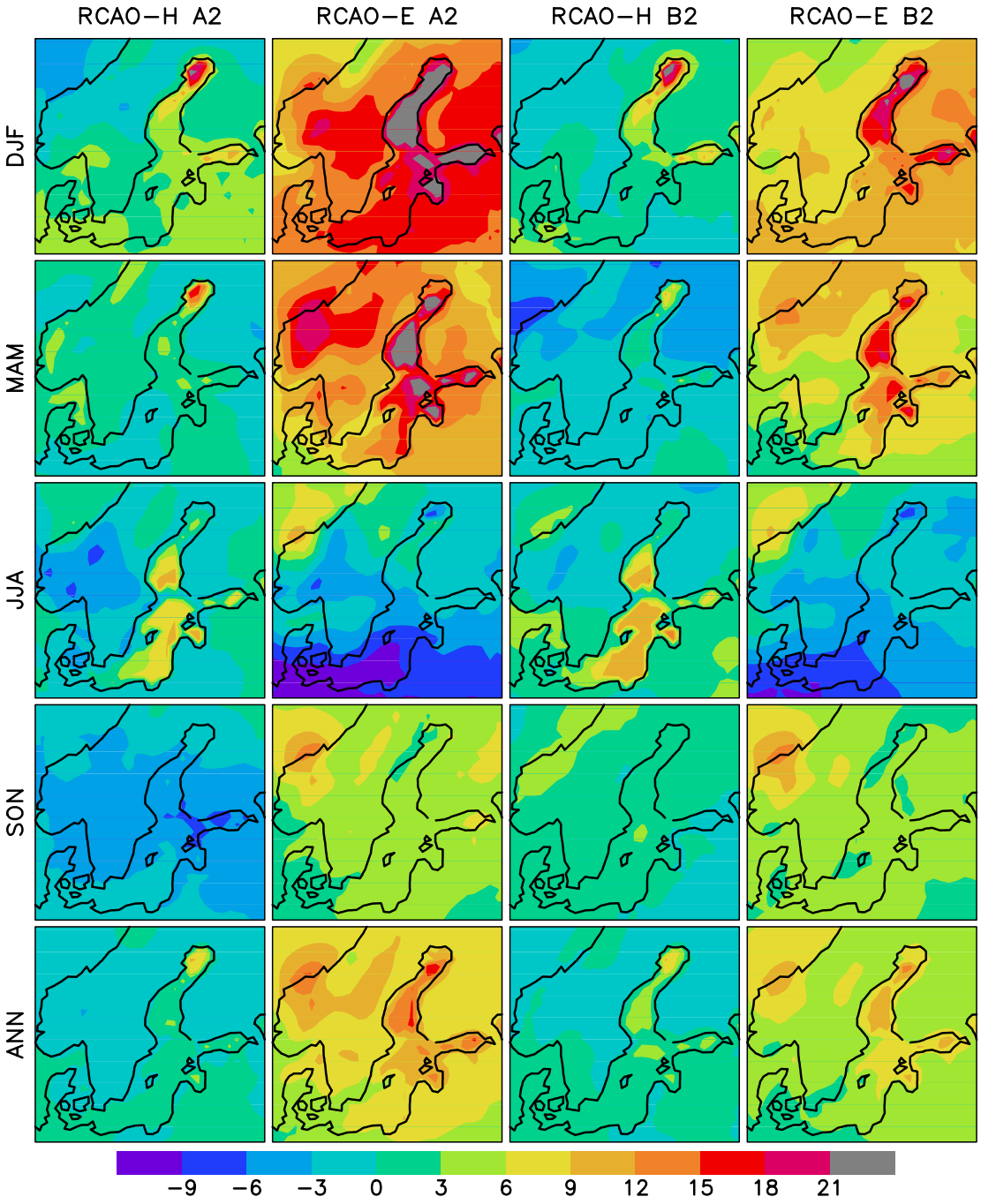

Figure 7. *Seasonal and annual changes in wind speed (percent differences from the corresponding control run) in the RCAO climate change simulations.*

Regardless of the emission scenario and driving GCM the strongest changes in the Nordic area appear over the Baltic Sea. Räisänen et al. (2003) suggested that changes in ice cover and sea surface temperature (SST) lead to decreased surface layer stability and thereby increased wind speed over the Baltic Sea. A comparison of the lapse rate between

the 2m level and the 925hPa pressure level confirmed this suggestion (not shown). The lapse rate in winter increases in the scenario simulations, implying less stable conditions. Also, the increase in lapse rate is largest over the same regions of the Baltic Sea as where the largest increases in 10 m wind speed are seen in Figure 7, i.e. the Bothnian Bay, the Bothnian Sea, and the Gulf of Finland. On the contrary, the increase in wind speed at 925 hPa (not shown), well above the surface layer, is uniform over the Baltic Sea in RCAO-H/A2 and RCAO-H/B2 and largest in the Baltic proper in RCAO-E/A2 and RCAO-E/B2. The lapse rate increases also during spring, but less than in winter. During summer the lapse rate increases in RCAO-H/A2 and RCAO-H/B2 while there is only little change in RCAO-E/A2 and RCAO-E/B2. This increase in the RCAO-H runs is in accordance with the local maximum in wind speed increase seen over the Baltic Sea in Figure 7. In fall there are almost no changes in stability in any of the simulations.

The change in wind is not just a change in wind speed as indicated in Figure 7 but also a change in wind direction. Figures 8 and 9 show the change in the seasonal averages of the westerly (u) and southerly (v) wind components. The strong increase in the north-south pressure gradient in RCAO-E during most of the year leads to a strong increase in the u-wind as seen in Figure 8. The fact that the u-wind increases more than the v-wind implies that the average wind direction becomes more westerly. In RCAO-H the changes in the u- and v-wind components are smaller and of similar size on an annual mean basis. It is only during summer that the directional changes in wind in RCAO-E and RCAO-H are similar with increasing westerly and decreasing southerly components.

In order to investigate how the wind climate is simulated to change on a more detailed temporal scale than just seasonal averages diurnal averages were studied. In Figure 10 probability distributions of diurnally averaged wind speeds at three locations around the Baltic Sea are presented. Shown are DJF conditions from the RCAO-E control and A2 runs to illustrate the strongest climate change signal in the four experiments. The increase in wind speed in Figure 10 is more or less uniform, i.e. the entire probability distribution is shifted to the right in the lower panels describing the future climate. In the other seasons as well as in the other climate change simulations the pattern is the same, i.e. generally uniform changes in the probability distributions.

In Figure 11 changes in wind speed at different percentiles are shown for the Baltic region. The plots indicate that the differences are rather small between changes in different percentiles implying a uniform change in wind speed. An exception seems to be the slightly larger increases at low wind speeds, particularly over parts of the Baltic Sea. However, these differences between the changes at low and higher wind speeds are just an effect of larger relative changes close to zero (calm conditions). In fact, the absolute change (in m/s) over the Baltic Sea is slightly larger for high than for low wind speeds (not shown). The almost uniform increase in wind speed shown here implies that the wind speed at extreme events is simulated to increase just as much as the mean. This is the case for all seasons and all four projections. However, the change in high wind speed should be considered as uncertain due to the models inability to simulate high wind speeds in the control climate case.

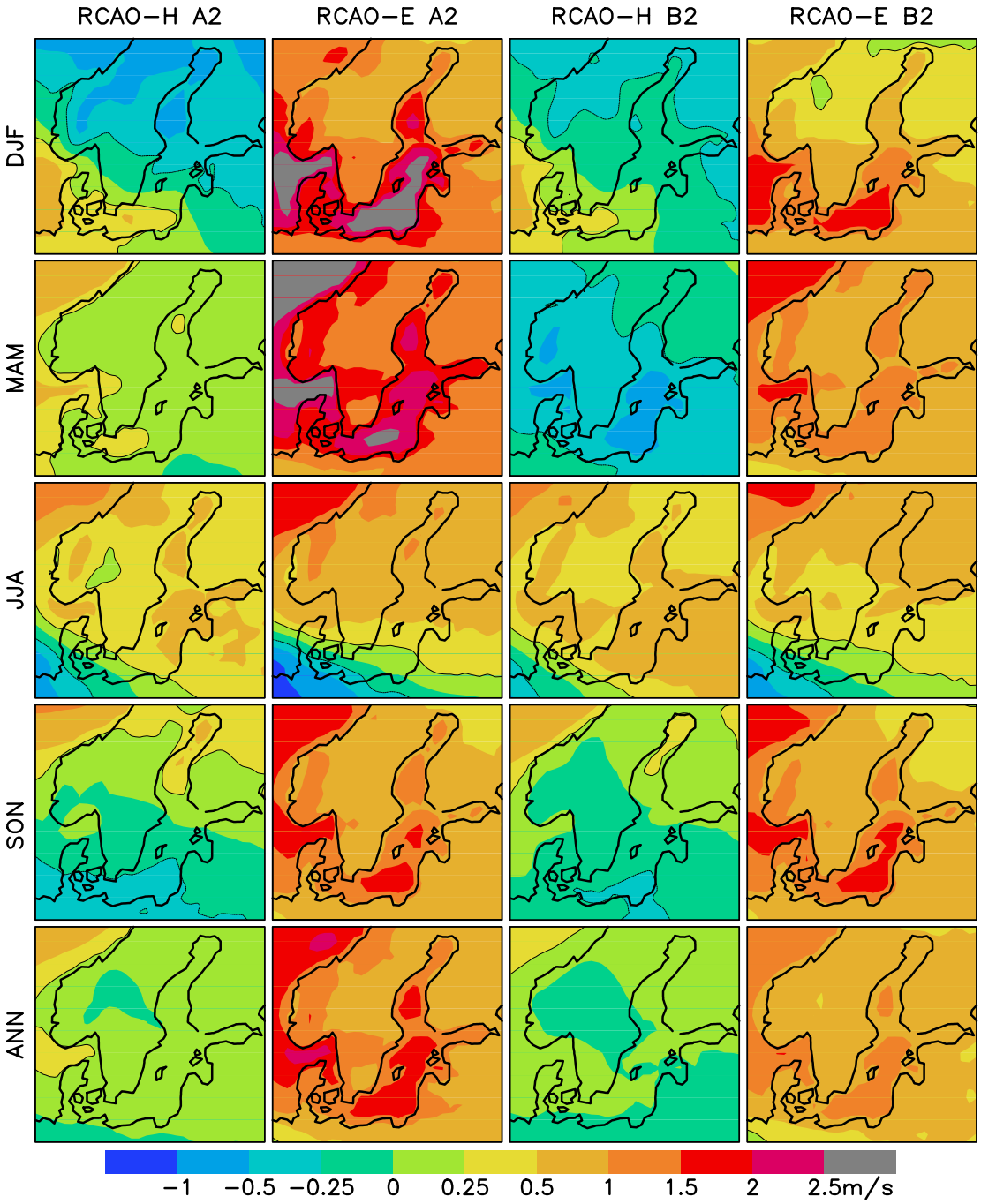

Figure 8. *Seasonal and annual changes in the westerly wind component (m/s) in the RCAO climate change simulations.*

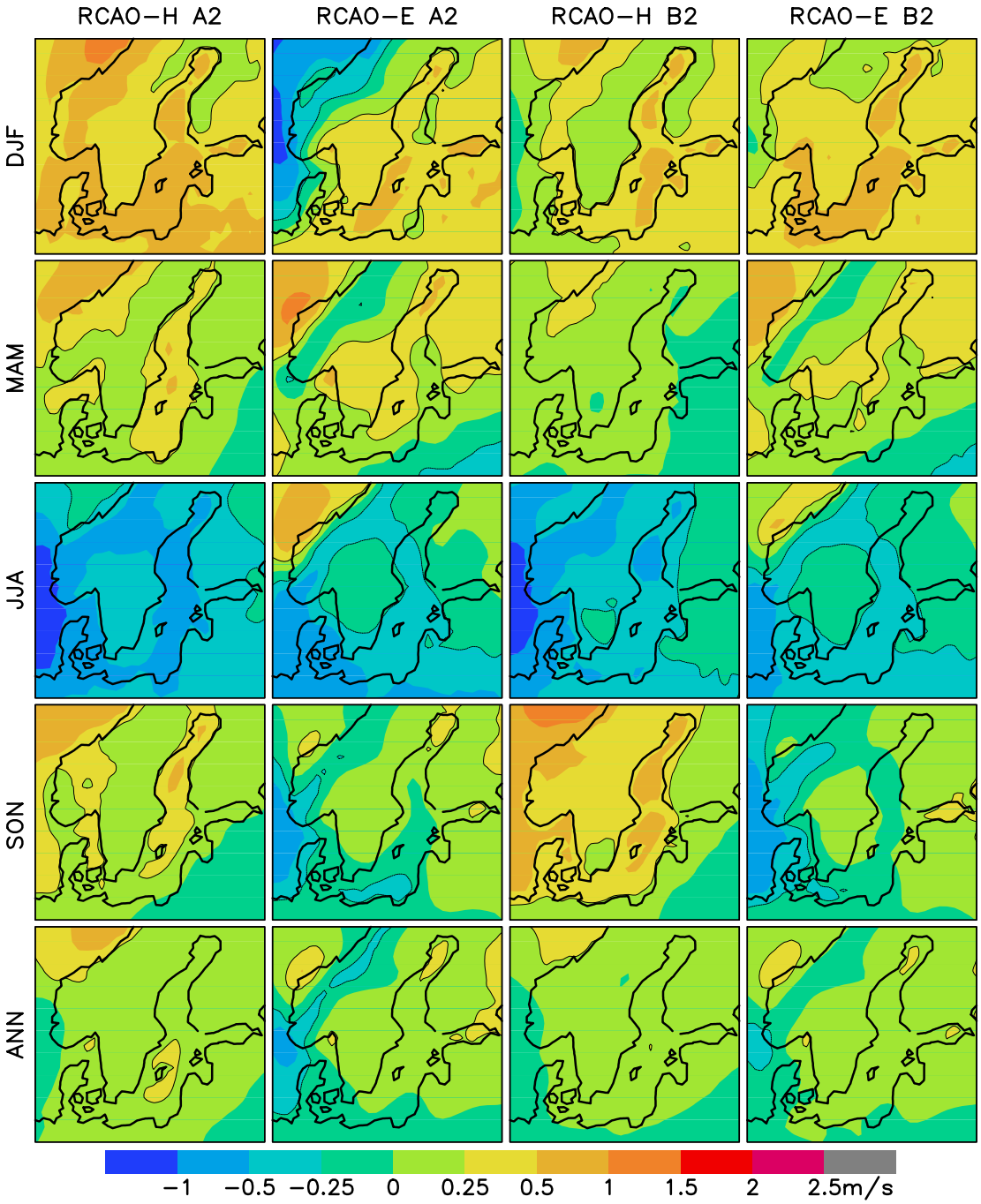

Figure 9. *Seasonal and annual changes in the southerly wind component (m/s) in the RCAO climate change simulations.*

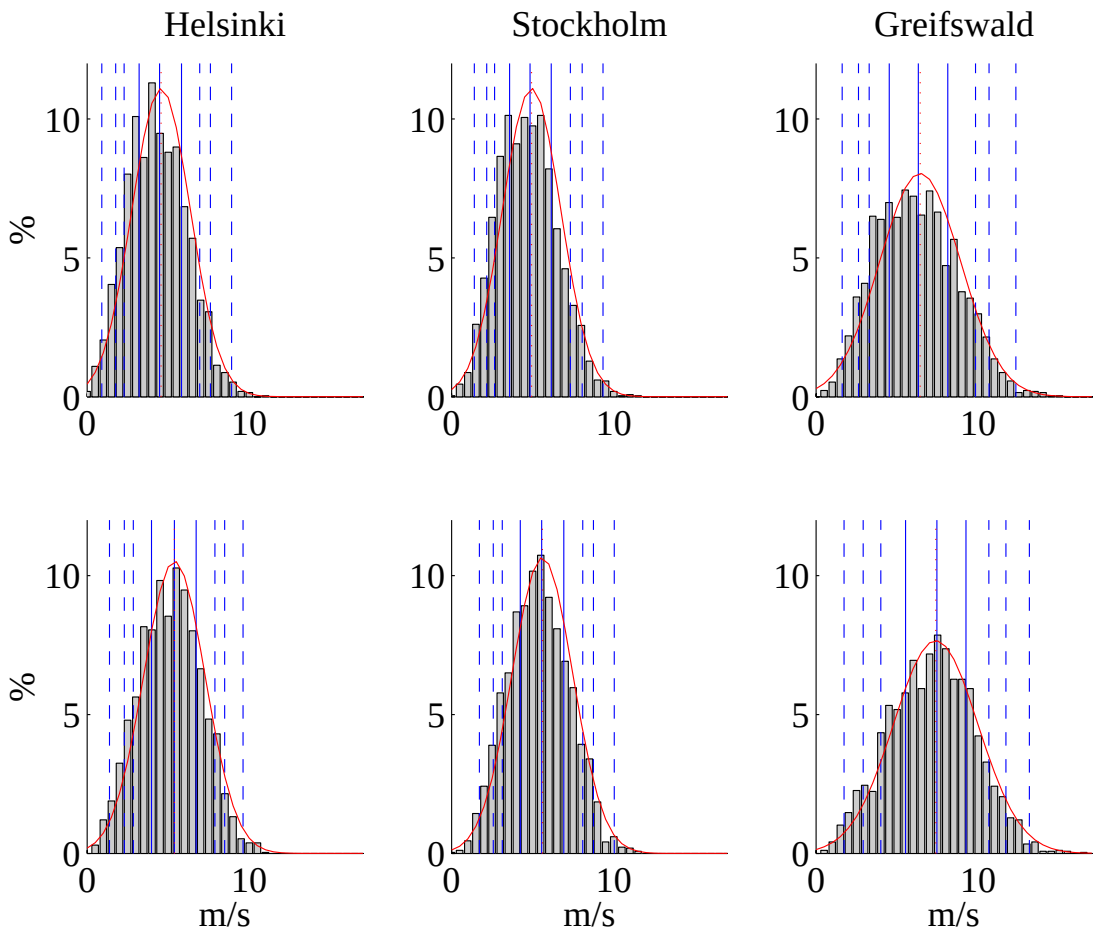

Figure 10. *Wintertime frequency (in %) histograms of wind speed in the RCAO-E control run (upper panels) and RCAO-E/A2 run (lower panels). The bars represent the actual distribution of the diurnally averaged data (N=2700 in each panel) with an interval of 0.5 m/s. The red dotted line is the mean and the red full line is a normal distribution with the mean and standard deviation taken from the actual distributions. The dashed and full blue lines are the percentiles (1st, 5th, 10th, 25th, median, 75th, 90th, 95th and 99th) of the distributions.*

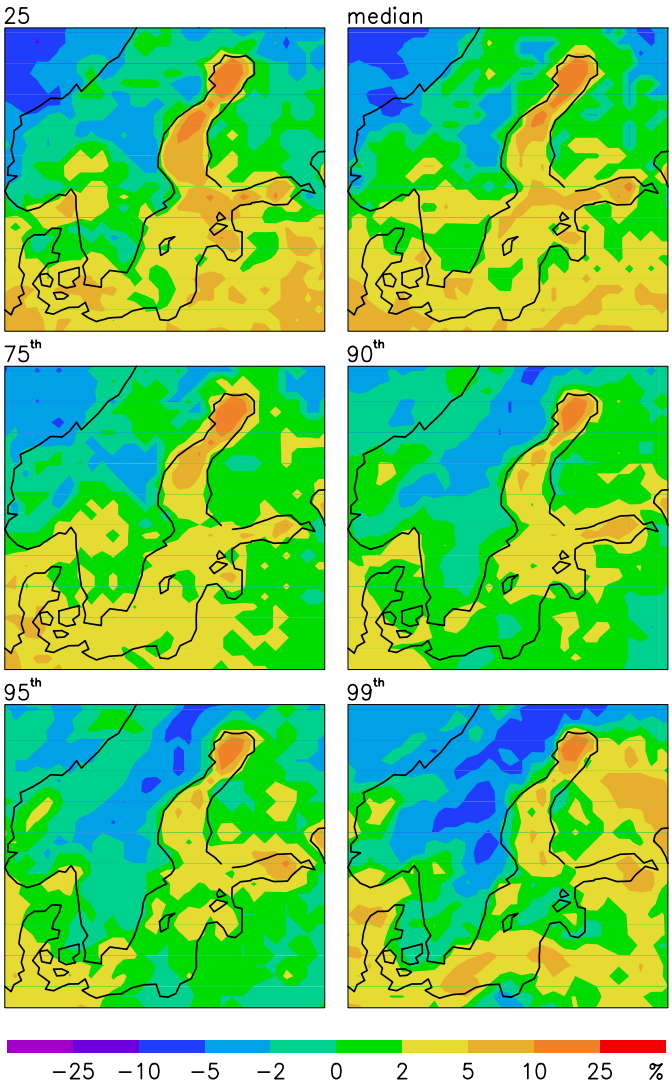

Figure 11. *Change in DJF wind speed at different percentiles (percent differences from the corresponding control run) in the RCAO-H/A2 climate change simulation.*

3.2 Sea level extremes

In Figure 12 the mean sea level in RCO-REF for the period 1903-1998 is shown. The mean sea level increases from the northern Kattegat toward the northern Bothnian Bay or toward the eastern Gulf of Finland by about 30 cm as a result of the prevailing westerly wind and of the decreasing salinity between Kattegat and the northern Bothnian Bay or the eastern Gulf of Finland. The largest monthly mean changes in all four scenario simulations were found in RCO-E/A2 (Fig. 13). However, even in this scenario simulation the maximum change of the median sea level in winter (December to February) is still smaller than 20 cm (Fig. 12). In this calculation land uplift and the global average sea level rise are not considered. The effect is purely based upon regional wind changes as described in section 3.1.2. In the RCO simulations approximately the same monthly mean sea level changes as in the RCAO simulations (Meier et al., 2004a; Figs. 5 and 6) were found. The small differences of the mean sea level changes between coupled and uncoupled scenario simulations of a few centimeters may be explained by the changing stratification during the longer integration in the uncoupled compared to the coupled simulations. In addition, in the RCO simulations (RCO-REF, RCO-H/B2, etc.) the wind speed at 10 m height was calculated from SLP (section 2.2), whereas in the RCAO simulations (RCAO-E, RCAO-H, etc.), the calculation of the 10 m wind speed was part of the boundary layer parameterization of the atmospheric model RCA.

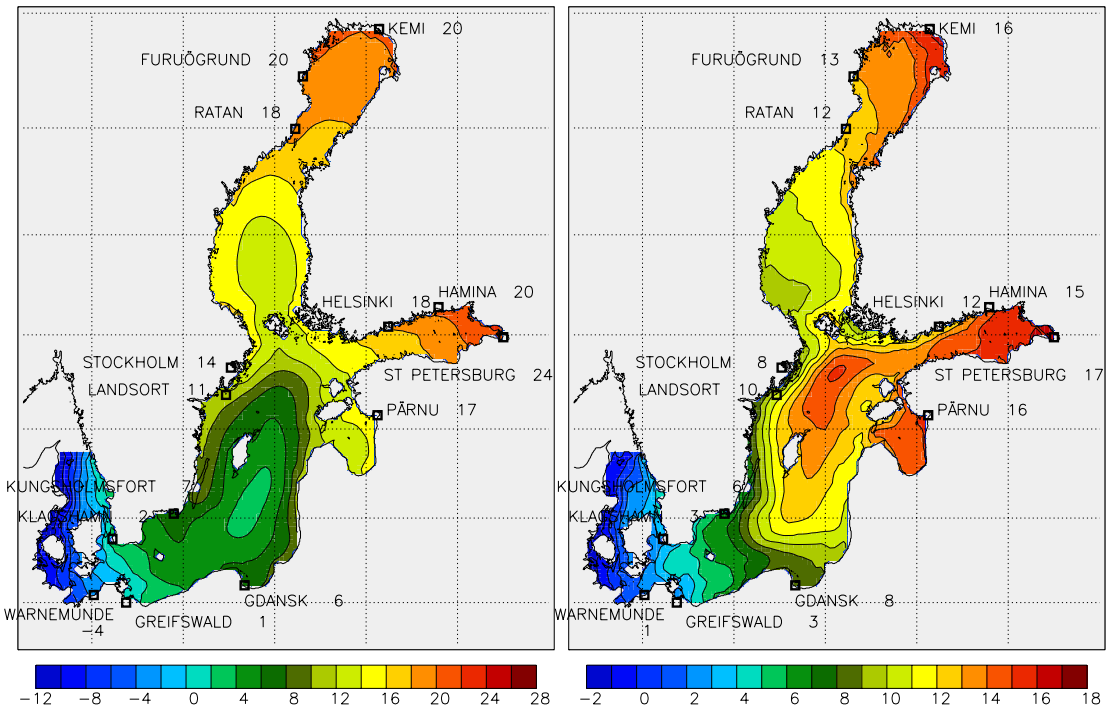

Figure 12. *Left panel: Mean sea level (in cm) of the hindcast simulation RCO-REF for 1903-1998 in the Nordic height system 1960 (NH60). Right panel: Change of the 50th percentile of the winter (DJF) sea level (RCO-E/A2 minus RCO-REF).*

The evolution of the monthly mean sea level changes (Fig. 13) follows that of the monthly mean wind speed changes (Meier, 2006; Fig. 2). In the scenario simulations driven by ECHAM4/OPYC3, RCO-E/B2 and RCO-E/A2, the largest monthly changes were found during February and March. In the scenario simulations driven by HadAM3H monthly mean changes are small and mainly not statistically significant. However, in June and July the sea

level changes are statistically significant at the 99% confidence level although the increases amount to less than 10 cm.

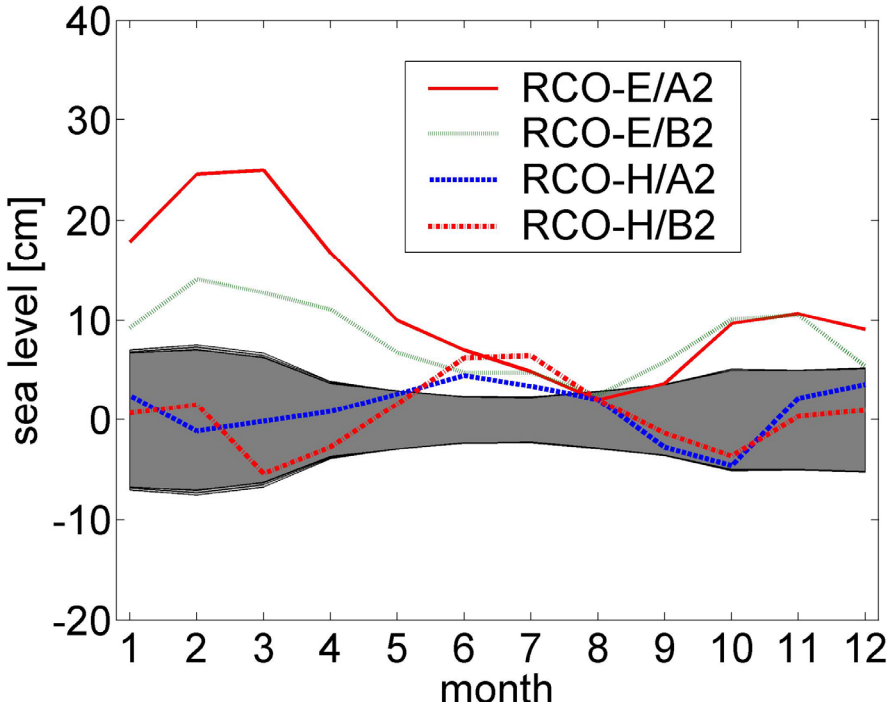

Figure 13. *Climatological monthly mean sea level changes (in cm) at Hamina in the Gulf of Finland between the periods 2071-2100 and 1961-1990. Shading indicates 99% confidence limits of internal variability. The location of Hamina is shown in Figure 12.*

Summarizing, wind induced monthly mean sea level changes are much smaller than the central value of the global average sea level rise of 48 cm of all global scenario simulations (Church et al., 2001). They are also smaller than the land uplift in the northern and central Baltic Sea. According to Ekman (1996) largest absolute land uplift rates of about 1 m per 100 years were found in the Bothnian Bay. Thus, the risk of flooding caused by wind induced monthly mean sea level changes is relatively small. In the following changes of sea level extremes are investigated.

In the scenario simulations with significantly increased west wind, sea level extremes increase more than the mean sea level. In Figure 14 the winter sea level changes in RCO-E/A2 at the 90^{th}, 99^{th}, and 99.95^{th} percentiles, and the maximum sea level changes are shown. Especially in the eastern part of the Baltic (i.e. Gulf of Finland and Gulf of Riga) the changes at the higher percentiles are much larger than the changes of the mean sea level (cf. Fig. 12).

In the following we will focus on the analysis of changing extremes with a 100-year return period because events with very high amplitudes are of special importance for spatial planning. In general, the agreement between 100-year surges calculated from model results of RCO-REF and 100-year surges calculated from available observations is satisfactory (Meier, 2006). However, at some selected locations the model failed to reproduce 100-year surges. These biases might be explained by unresolved topographical details within RCO, different time periods of available observations, or different time resolutions. Due to the coarse model resolution of 6 nautical miles, volume transports through the Danish straits on synoptical or

smaller time scales are overestimated. Consequently, storm surges in the western Baltic (Belt Sea, Arkona Basin, and Bornholm Basin) caused by north-easterly winds are underestimated. In Figure 15 100-year surges in NH60 are depicted. For comparison with other studies of observed sea level extremes, in Figure 16 also the 100-year surges above the mean sea level 1903-1998 are shown. The eastern coasts of the Gulf of Finland and of the Gulf of Riga are exposed to non-linear piling up of the water during storm surges.

Changes of the 100-year surges differ considerably between the performed scenario simulations (Fig. 15). The results of the scenario simulation RCO-H/B2 are not shown because the changes are very small (< 22 cm) and in most areas statistically not significant. In the scenario simulations driven by ECHAM4/OPYC3 the west wind during winter is significantly intensified (Fig. 8) causing considerable changes of the 100-year surges in the Gulf of Finland, Gulf of Riga, and in the north-eastern Bothnian Bay (Fig. 15). In RCO-E/A2 relative wind speed changes averaged for the Baltic Sea amount to 33% in March (Meier, 2006; Fig. 2). As a consequence, in RCO-E/A2 the simulated 100-year surges in St.Petersburg in the eastern Gulf of Finland and in Pärnu in the north-eastern Gulf of Riga increase compared to present climate with 68 and 63 cm, respectively. Quoting the full range of our scenario simulations can give an idea of the uncertainty of the calculated changes. We found that the 100-year surges in St. Petersburg and Pärnu change between 6 and 68 cm and between 2 and 63 cm, respectively. The ensemble average changes of the 100-year surge amount to 32 and 27 cm, respectively. In Stockholm the 100-year surge will only increase between 1 and 26 cm with an ensemble average of 11 cm. The depicted changes of surge heights are statistically significant at the 99% level except in the Kattegat area. However, in RCO-H/A2 calculated changes are not significant in the Belt Sea and in parts of the Arkona Basin.

However, in addition to the changing regional wind field land uplift and the global sea level rise have to be considered. In Figure 16 these three factors have been combined as mentioned in section 2.2. Three projections (`low case´, `ensemble average´, and `high case´) have been selected to characterize the range of uncertainties due to regional wind driven effects and global sea level rises. According to these calculations the 100-year surges in St. Petersburg and Pärnu will increase relative to the mean sea level 1903-1998 between 0 and 141 cm and between –9 and 130 cm, respectively. The ensemble average changes amount to 64 and 55 cm, respectively. In Stockholm the 100-year surge changes between –51 and 53 cm with an ensemble average of –1 cm. The risk of flooding is here assessed as relatively small because even in the `high case´ projection the 100-year surge of 168 cm will not exceed the critical height of the jetty walls which is 180 cm or higher (Meier et al., 2004a).

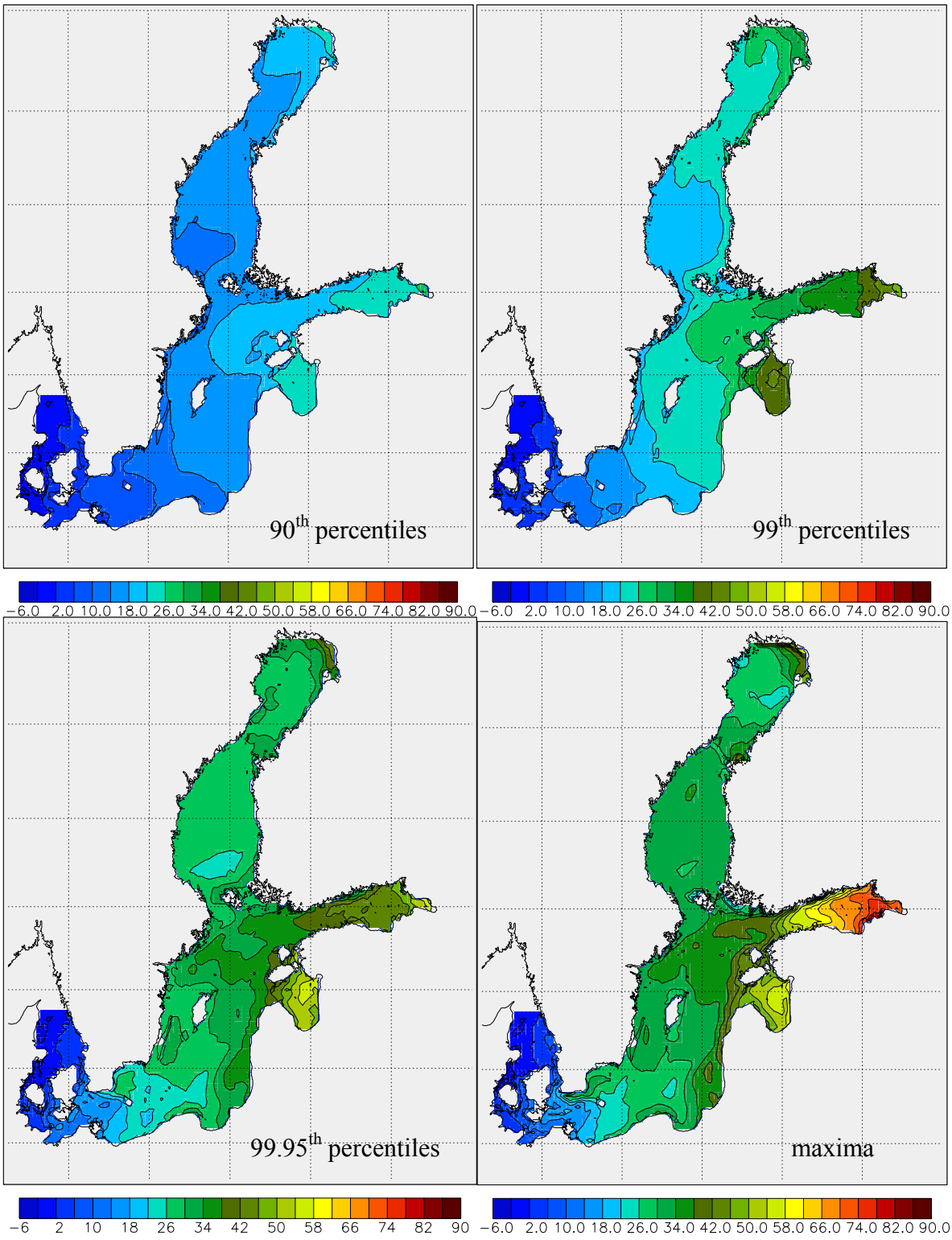

Figure 14. *Changes of the winter (DJF) sea level (in cm) at different percentiles and of the maximum between the RCO-E/A2 simulation (2071-2100) and the reference experiment RCO-REF (1961-1990).*

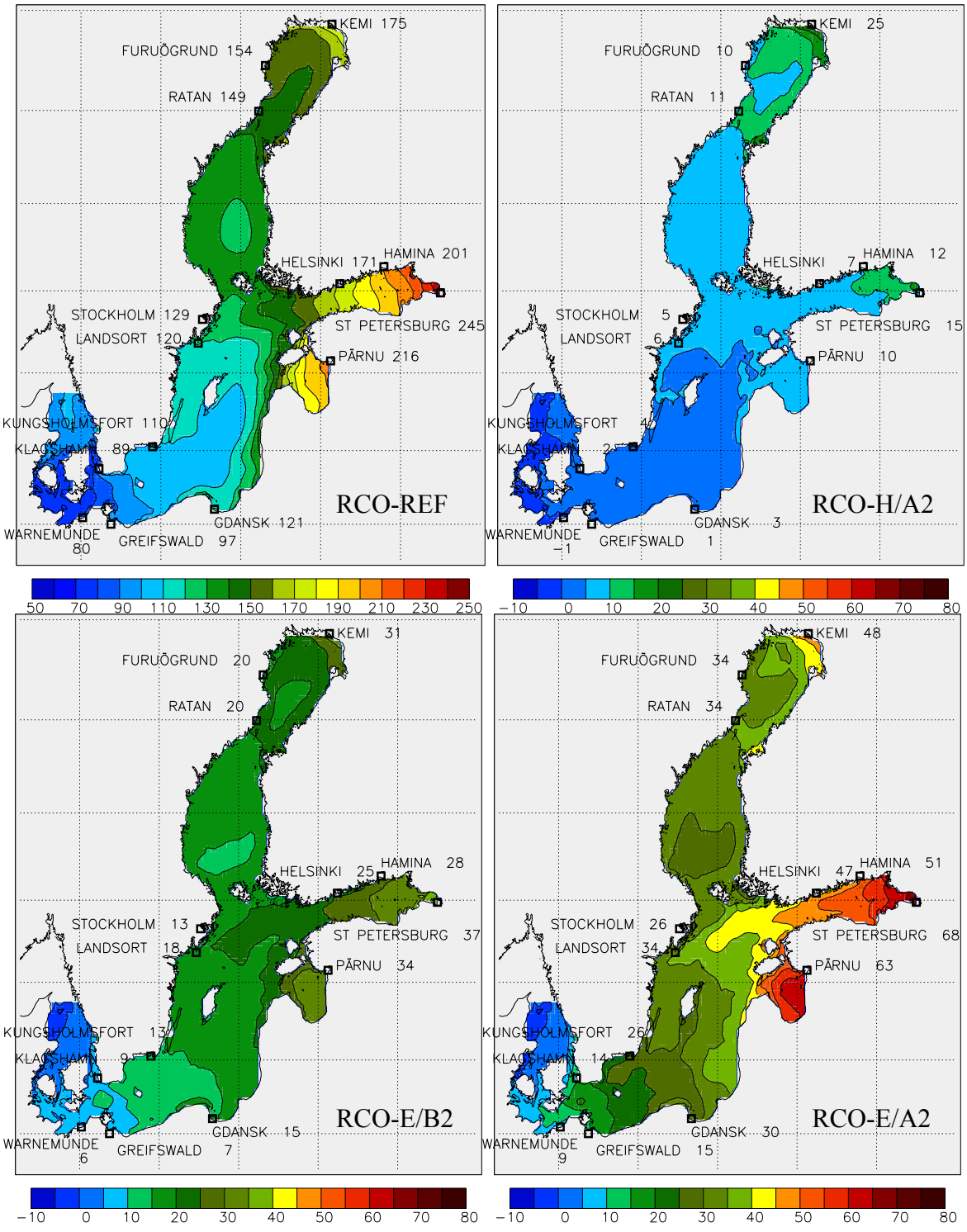

Figure 15. *100-year surges (in cm) in the hindcast experiment (RCO-REF) in the Nordic height system 1960 (NH60) and their changes in various scenario simulations.*

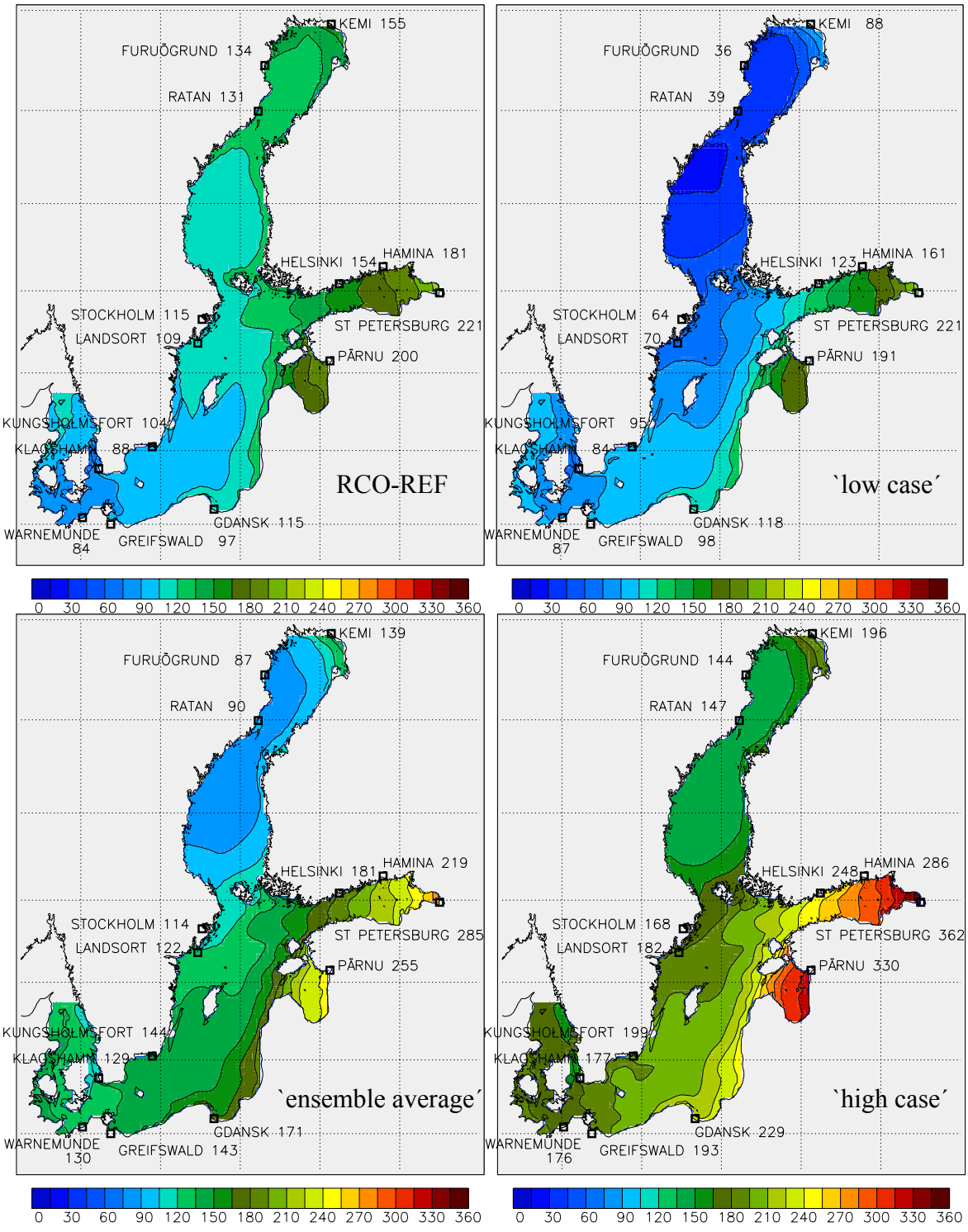

Figure 16. *100-year surges (in cm) in the hindcast experiment (RCO-REF) and in three selected regional scenario simulations relative to the mean sea level 1903-1998: `low case´ projection (RCO-H/B2) with a global average sea level rise of 9 cm, `ensemble average´ projection with a global average sea level rise of 48 cm, and `high case´ projection (RCO-E/A2) with a global average sea level rise of 88 cm. In the scenario simulations land uplift during 110 years (1961-2070) is considered. The figure is taken from Meier (2006, Fig. 23) with kind permission of Springer Science and Business Media.*

3.3 Hydrological modeling results

All of the RCAO climate scenario simulations indicate an increase in the future mean temperature over the Lake Mälaren region, with annual values ranging from +2.5ºC to +4.8ºC, as shown in Table 6. Precipitation shows a corresponding annual increase of about +4% to +15%, as does evapotranspiration from about +9% to +22%. These changes, when interpreted with the hydrological model, resulted in a decrease in annual inflow volume for the RCAO-H scenarios (-4% to -7%) and an increase for the RCAO-E scenarios (+2% to +8%). This is based on comparison to hydrological model results summarized for the reference period 1964-1990, which overlaps the RCAO control period simulations (1961-1990). The reference period is somewhat shorter than 30 years because data are not available for the beginning of the 1960s.

Table 6. *Mean annual change in temperature, precipitation and evapotranspiration from RCAO climate scenario simulations for the Lake Mälaren drainage basin. The change in mean annual inflow to the lake resulting from HBV hydrological modeling is also shown, as compared to the 1964-1990 reference simulation.*

Variable	RCAO-H/A2	RCAO-H/B2	RCAO-E/A2	RCAO-E/B2
Temperature (°C)	3.8	2.5	4.8	3.7
Precipitation (%)	6.3	4.2	14.9	13.0
Evapotranspiration (%)	14.4	9.3	22.1	15.7
Inflow (%)	-6.7	-4.3	2.4	8.4

Regarding changes in seasonality, the hydrological impact simulations showed tendencies towards higher autumn and winter inflows, although the magnitude of the changes differed depending on scenario, as shown in Figure 17. Winter precipitation, which in the reference simulation (1964-1990) accumulated as snow, fell to a large extent as rain in the future simulations, resulting in a reduction of the spring peak flow in the mean hydrographs. Inflow during summer was considerably lower for all future simulations. For comparison to more recent conditions, hydrological simulations from the years 1991-2002 are also plotted in Figure 17. Compared to the reference simulation, they show much higher inflows during winter months and a considerably lower annual peak inflow.

The changes in seasonality were also reflected in the results from a frequency analysis using the Gumbel distribution. The inflow corresponding to a return period of 100 years was evaluated on an annual basis, as well as for spring (defined as January-July) and autumn (defined as August-December), as shown in Table 7. The projections show a decrease in the magnitude of the 100-year spring inflow and an increase in the 100-year autumn inflow. The change was so large that the scenario simulations also show a shift from the highest flood in the spring to instead having the highest flood in the autumn. The projected return period for the 100-year inflow of 1964-1990 was 300-400 years (representing 2071-2100).

Inflow volumes are more critical for water levels in large lakes than short duration peak flows. Table 8 further quantifies the results shown in Figure 17 by summarizing mean inflows for two characteristic three-month periods. These periods represent the two periods where peak inflows typically occur for the reference period. The table shows that for three of the scenario simulations, the period with higher mean inflows (representing higher inflow

volume) changes from spring months (March-May) to cold season months (November-January). It can also be noted that during recent years (1991-2002), mean flows do not differ much between the two periods.

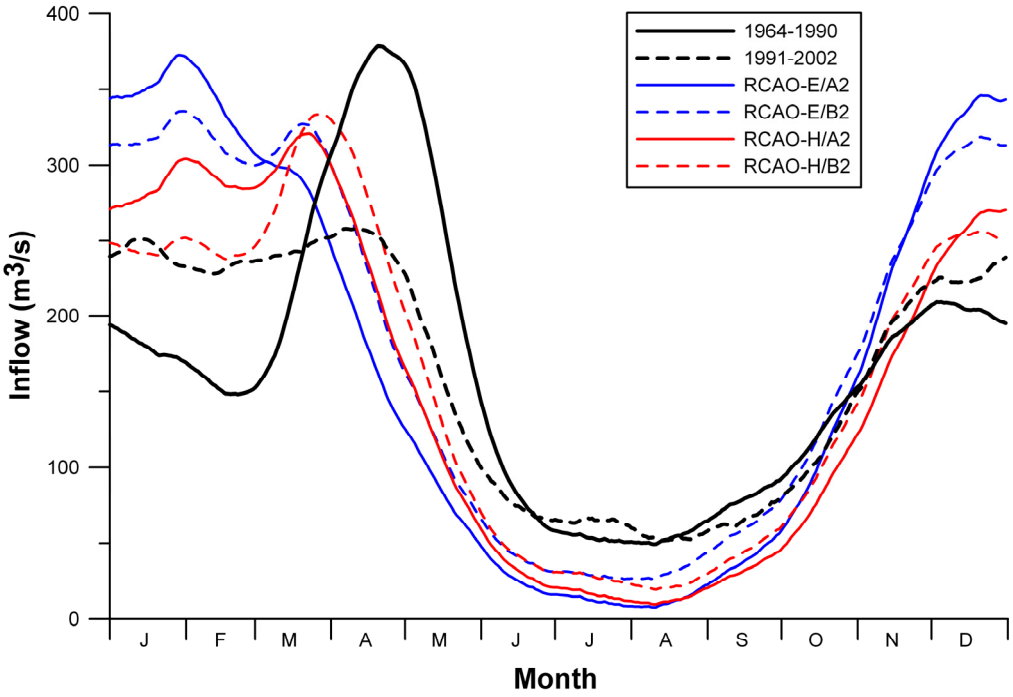

Figure 17. *Modeled seasonal river inflow to Lake Mälaren from HBV simulations using observations for the reference period (1964-1990) and four projected climate change scenarios (representing 2071-2100). Also included are HBV simulations using observations from a more recent period (1991-2002). Shown are smoothed daily means over the modeling period.*

Table 7. *Percent change in peak magnitude for the 100-year inflow to Lake Mälaren from four climate change scenarios, as compared to the 1964-1990 reference simulation. Spring is defined here as January to July and autumn is defined as August to December.*

Period	RCAO-H/A2	RCAO-H/B2	RCAO-E/A2	RCAO-E/B2
Spring (%)	-13	-15	-16	-14
Autumn (%)	15	19	51	39
Year (%)	-14	-15	-12	-12

Table 8. *Mean inflow to Lake Mälaren over two 3-month periods that represent the two peak inflow periods characteristic for the reference simulation (1964-1991). These are November to January and March to May.*

Period	ref 1961-1990	1991-2002	RCAO-H/A2	RCAO-H/B2	RCAO-E/A2	RCAO-E/B2
Nov-Jan (m^3s^{-1})	189	221	238	231	306	289
Mar-May (m^3s^{-1})	280	218	217	235	186	220

3.4 Lake discharge modeling results

To confirm that the lake discharge model could reasonably represent actual operations, it was first tested with observations as input. The high inflow situation from the year 2000 was chosen as a case study. Results are shown in Figure 18. As seen in the plot to the left in the figure, operations can be simulated with good accuracy by the model as demonstrated by the close match between simulated and observed water levels. The maximum level reached was 473 cm, with a simulated total outflow of 851 m^3s^{-1}. This was achieved by knowingly violating the guidelines for releases that are stipulated in the Water Court Decree. Specifically, releases were begun at some locks before the specified water levels were reached. In addition, the flow capacity at both Hammarby and Södertälje locks were allowed to exceed the stipulated 70 m^3s^{-1} limit. These violations were also made in reality, so the simulations mimic the actual operations.

If the Water Court Decree had been strictly followed during this event, the water level for Lake Mälaren would have reached higher levels. This was reproduced with a simulation by the lake discharge model as shown by the red curve in the plot to the right in Figure 18. As a simple sensitivity study, the observed water levels in the Baltic Sea were increased by 46 cm, which resulted in the blue curve on the same plot (to the right in Figure 18). The corresponding maximum water levels for these two cases are 478 cm (maximum 818 m^3s^{-1}) and 483 cm (maximum 802 m^3s^{-1}), respectively.

For the investigation of the influence of climate change on water levels in Lake Mälaren, the hydrological results described in section 3.3 were used as inputs to the lake discharge model. The analysis focused on the SRES-A2 scenarios. Figure 19 shows results from both the RCAO-H/A2 and RCAO-E/A2 scenario simulations. These projections mimic the actual operations that occurred during the 2000 event, which means that the Water Court Decree was violated. As seen in the figure, the water level rose to 478 cm (maximum discharge of 864 m^3s^{-1}) for the RCAO-H/A2 scenario simulation and 515 cm (maximum discharge of 900 m^3s^{-1}) for the RCAO-E/A2 scenario simulation.

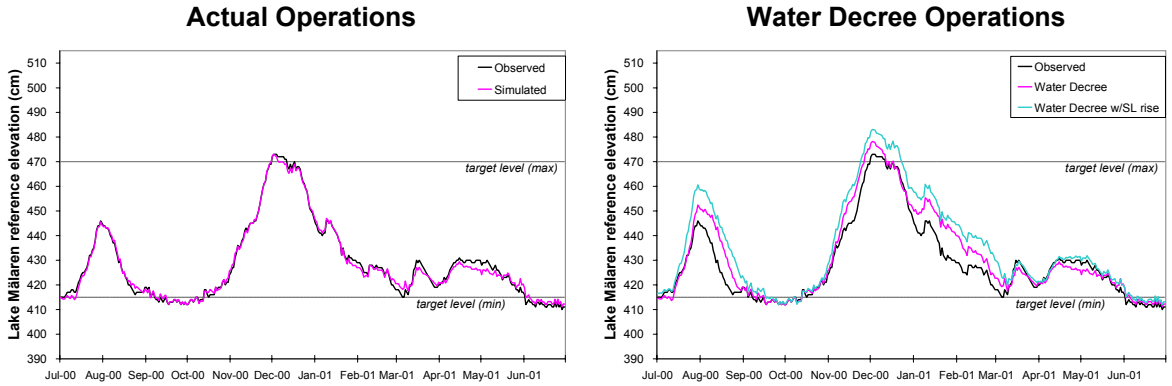

Figure 18. *Water level in Lake Mälaren resulting from lake discharge modeling of actual conditions for the high water event in December 2000. Shown to the left are simulated actual operations. Shown to the right are simulated operations that strictly follow the water decree for observed Baltic Sea level and for an increase in Baltic Sea level of 46 cm. The desired operational water levels for high and low flow conditions are identified as "target levels" on the plot.*

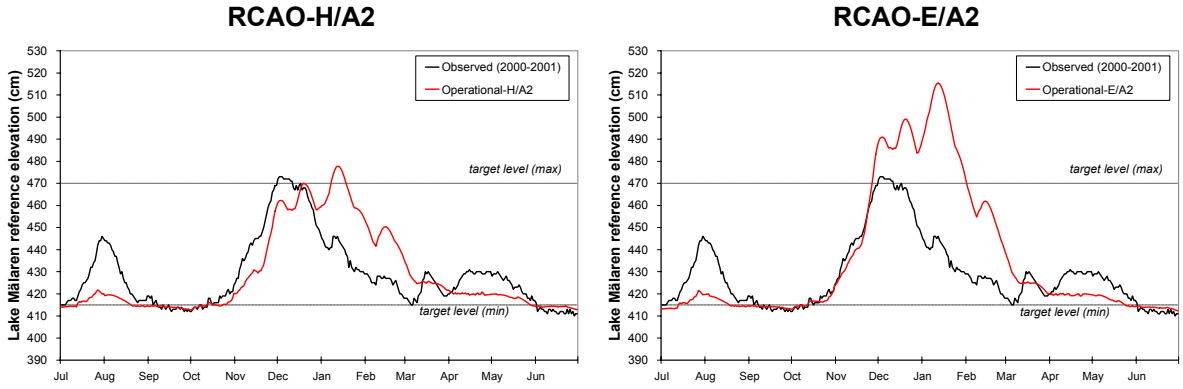

Figure 19. *Water levels in Lake Mälaren from lake discharge modeling of future climate conditions using the operational rules that mimicked actual conditions (i.e. as in the plot on the left in Figure 18). Results are shown for both the RCAO-H/A2 scenario simulation (left) and the RCAO-E/A2 scenario simulation (right). These projections represent the high water event from the year 2000 modified with the climate change scenarios.*

If the Water Court Decree were to be strictly followed for the changed climate conditions, the resulting water levels for Lake Mälaren would be as shown in Figure 20. This figure shows results using both observed Baltic sea levels and sea levels with a 46 cm increase according to the climate scenario simulations. The resulting levels are 478 cm (maximum 816 m^3s^{-1}) and 520 cm (maximum 981 m^3s^{-1}) for existing sea level, and 490 cm (maximum 806 m^3s^{-1}) and 527 cm (maximum 976 m^3s^{-1}) for increased sea level for the RCAO-H/A2 and RCAO-E/A2 scenario simulations, respectively. Note that the resulting maximum Mälaren water levels for RCAO-H/A2 using observed sea levels are the same regardless of whether actual (Fig. 19) or the Water Court Decree (Fig. 20) operating rules are used.

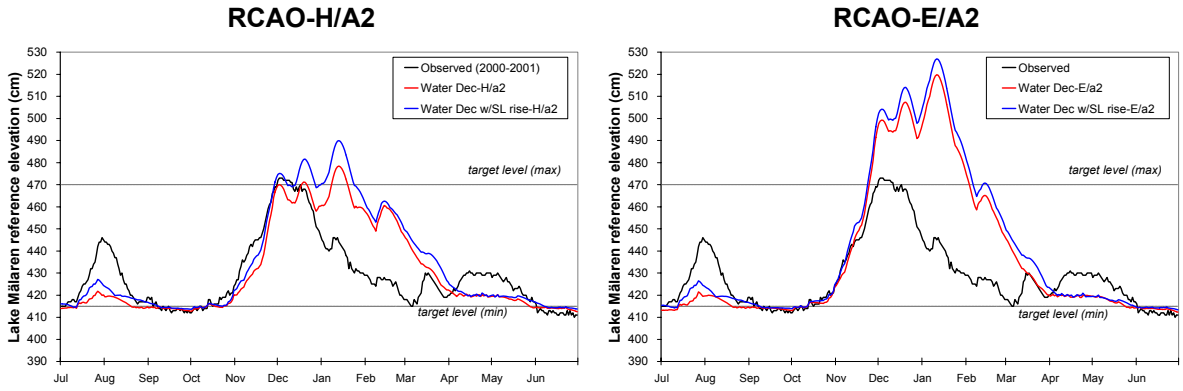

Figure 20. *Water levels in Lake Mälaren from lake discharge modeling of future climate conditions with strict adherence to the water decree (i.e. as in the plot on the right in Figure 18). Shown in red are results with observed Baltic Sea level and in blue for an increase in Baltic Sea level of 46 cm. Results are shown for both the RCAO-H/A2 scenario simulation (left) and the RCAO-E/A2 scenario simulation (right). These simulations represent the high water event from the year 2000 modified with the climate change scenarios.*

Analysis of the required outflow capacity that would keep Lake Mälaren water level from exceeding 470 cm for this event was also performed. These results are shown in Figure 21. The required outflow capacity was 933 m^3s^{-1} for the RCAO-H/A2 scenario simulation and

1237 m^3s^{-1} for the RCAO-E/A2 scenario simulation. Although the desired water level was not exceeded, it can be seen in the figure that long periods of substantially high water levels still occurred. For instance, the periods that the water level exceeded 450 cm and 460 cm are up to twice as long for the future climate than for observations of the actual event.

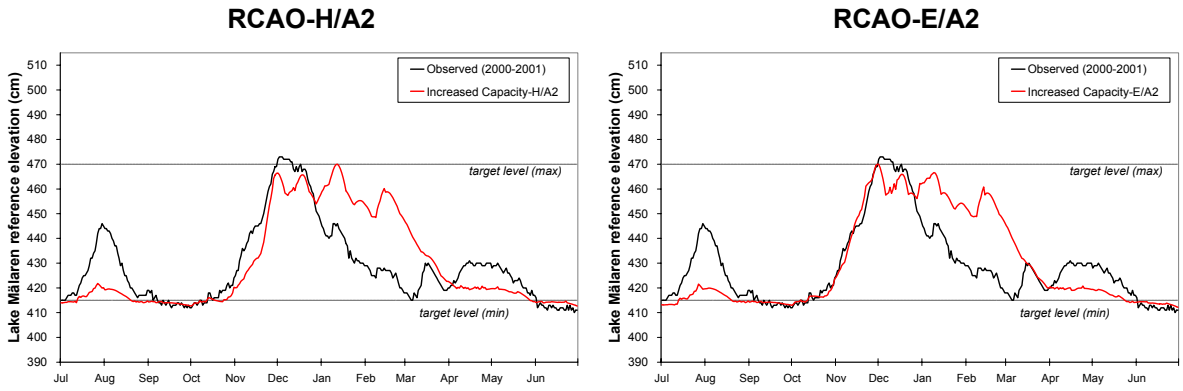

Figure 21. *Water levels in Lake Mälaren from lake discharge modeling of future climate conditions with increased outflow capacity from the lake. No increase in sea level was assumed. Results are shown for both the RCAO-H/A2 scenario simulation (left) and the RCAO-E/A2 scenario simulation (right). These simulations represent the high water event from the year 2000 modified with the climate change scenarios.*

3.5 Flood prone areas in the Lake Mälaren region

The analysis of potential flood prone areas around Lake Mälaren started with a regional overview analysis of the flooding situation in the region. Then two local case studies were made where either large areas were affected or important infrastructure was at stake. The areas chosen were Ekerö, a typical rural municipality in the vicinity of Stockholm, and the City of Stockholm itself with high urban densities and crucial infrastructure

Due to the uncertainty associated with evaluating climate change impacts (Gardelin et al., 2002), no single value can be placed on how inflows to Lake Mälaren will change in the future. This fact, combined with different future operating strategies for regulating outflow from the lake, leads to a range of potential lake levels for future conditions, as presented in section 3.4. Rather than trying to map all of the possibilities, it was decided to analyze impacts of floods from the two flood situations used in the GIS assessments, the 100-year flood (+0.65 m) and the maximum probable flood (+1.48 m) defined by previous studies (SRV, 2001), see section 2.4. These cases can be used as an index for comparison to future water level projections.

3.5.1 Overview analysis

Flooding around Lake Mälaren, both for the present and the future, is more sensitive to river inflow changes than to changes of the Baltic Sea levels (section 3.4). The current outflow capacity of the combined locks and floodgates is today insufficient for the extreme events of the present climate and thus even for the potential increases for future climate conditions as described in section 3.4. This lack of outflow capacity places the shoreline communities of the Stockholm-Mälar region at risk for potential flooding during high flow events.

The results of the overview GIS assessment identified those areas that needed to be further assessed in order to analyze risks and vulnerabilities (not shown). The regional map indicated that basically all municipalities around Lake Mälaren were subject to potential flooding risks. Two were selected for the further assessment in the project (Ekerö and Stockholm). The analysis on effected land use type is based on today's conditions and does not take into account possible changes in land use during the century. It is important to bear in mind that such changes most likely will occur.

3.5.2 Case study Ekerö

Ekerö comprises four major islands with two major settlements and many smaller communities and farms. It has approximately 23,000 inhabitants. This municipality is especially exposed to flooding events due its morphology. Large areas are former lake bottoms that have dried out due to the steady land uplift (0.4 m in 100 years). Large parts of the municipality's land area (213 km^2) are either open areas, i.e. natural zones, nature protection zones, or agricultural areas.

The conducted GIS assessment showed that at a lake level of +0.65 m 5% of the land of Ekerö would be flooded (Fig. 22, Tab. 9). However, high water levels are quite common for Ekerö and people are used to the fact that larger areas stand under water especially during late winter and early spring. Most of these concerned areas are not used for human activities and such flooding events at this level do not bring any harmful effects.

At a level of +1.48 m around 9% or 18 km^2 of the municipality's land area is flooded (Fig. 22, Tab. 9). Arable land, pastureland, and woods are mostly affected. Some housing areas, mostly summer cottage areas, and some industrial estates would be affected. However, it is primarily a shipyard in the northern part of Färingsö, which would be most affected. The very low-lying northern parts of Färingsö would become small islands (particularly areas of Händaskär and Hända) in the event of this level, corresponding to the maximum probable flood.

Mostly agricultural land and open spaces as well as forests would be subject to flooding. Industry and housing areas are mostly unaffected by flooding (Table 9).
The vulnerability of Ekerö is rather low despite the extent of flood prone areas as shown in Table 9. There exists a certain isolation risk for some parts of the islands, which only have one access road. Many roads have embankments that are situated on a higher level than the surrounding land. These embankments are, however, endangered by possible destabilisation. High water levels would apparently not greatly affect technical infrastructure such as the sewage plant, telecom, electricity facilities and car ferry harbours. Even though higher floods influence many small marinas, the risks for damage are small.

Basically all farm buildings are situated on higher land sites where there is no flooding risk. The situation for up to 100 summer cottages is different as they are situated on low sites close to the water. At a water level of 1.48 m, 60 permanent housing estates might be affected. However, the GIS based assessment cannot estimate the extent of such damages.

Figure 22. *Overview map of Ekerö municipality showing the flood risk areas. The detailed map is shown in Figure 23.* ***Figures 22 and 23 are not available in this pdf edition due to copyright laws. They are available in the printed edition of the report.***

Table 9. *Affected land use types (in ha) due to flooding in Ekerö municipality.*

Land use type	+0.65 m (ha)	% of total area	+1.48 m (ha)	% of total area	Total area (ha)
Housing	1	0	3	1	340
Industry	1	4	4	15	27
Arable land	501	8	797	13	6 195
Pastureland	111	8	484	14	3 500
Conifer woods	192	2	394	4	10 737
Hard woods	111	21	174	34	518
Total	1 102	5	1 856	9	21 316

One of the water protection areas of the municipality, Northern Munsö, is quite close to Lake Mälaren. It could be affected through a higher flooding event due to infiltration of surface water into the ground water. The water quality in private wells can also be impaired. Only 17,000 of a total 23,500 estates are part of the municipal sewage and fresh water supply system. How the private sewage systems would be affected depends on their location and state. There is a risk that these systems do not work during and after a flooding event. Ekerö's farmers may also experience problems from flooding due to high moisture levels that hinder fieldwork during springtime (Fig. 23).

Figure 23. *Ekerö centrum and Tappström, one of two major settlements of the municipality.* ***Figures 22 and 23 are not available in this pdf edition due to copyright laws. They are available in the printed edition of the report.***

3.5.3 Case study Stockholm

The City of Stockholm has a very dense urban environment with many crucial infrastructure facilities and many housing areas along the lake shores. The city comprises seven major densely populated islands and has a total of 758,000 inhabitants, whereof a large part has dwellings and apartments directly at the waterfront. Many low lying areas in Stockholm are situated in potential floodplain areas of the lake (Fig. 24). Flood risk areas in the city center of Stockholm are of particular interest as the area is very densely populated and has many important infrastructure facilities (Fig. 25).

At a water level of +0.65 m the entrance hall of the metro station at Gamla Stan would be endangered and malfunction of certain parts of the grey water sewage system near the lake's shoreline would occur. At a water level of +1.48 m crucial facilities, such as central streets near the Central Station, the metro station at Gamla Stan, and surrounding street areas would be endangered.

In the high level case also several marinas, leisure facilities, walkways and parks along the shores would be flooded. In some parts of the city residential areas (e.g. Hässelby and the island Stora Essingen) and garden cottage areas (e.g. Ulvsunda) are affected. Several estates with both business and private owners would be affected but likely not the buildings themselves.

A rough analysis of Stockholm's large tunnel system (telecom, electricity, water, sewage, metro, broad band) made by the city's expert group for tunnels showed that there will evidently be risks if the water level rises to the maximum probable flood level. As the tunnels are owned and operated by various stakeholders, and as the communication on risks is limited due to confidential information, this study cannot say anything concrete about risks and vulnerability.

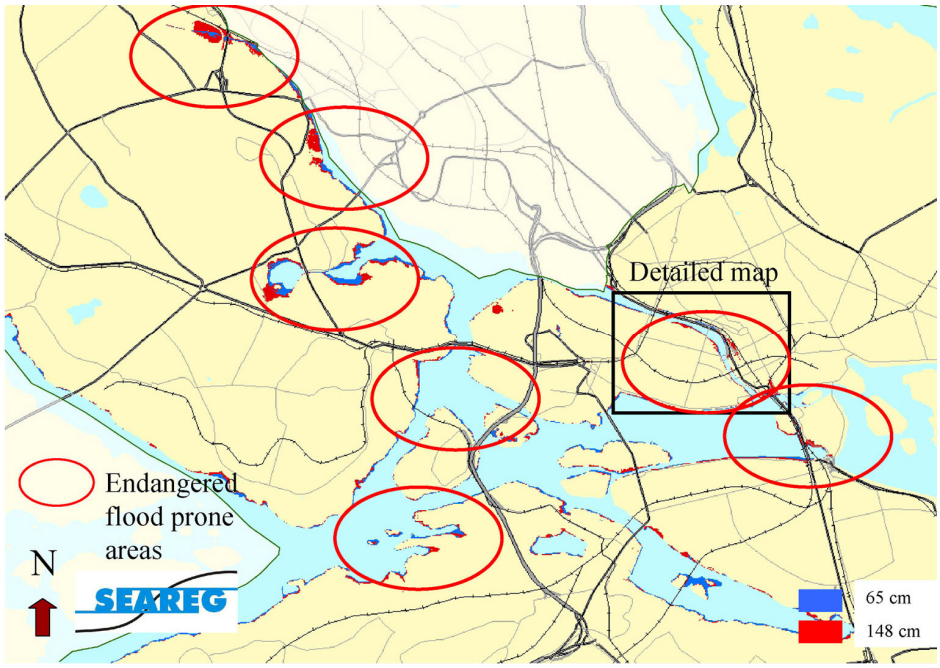

Figure 24. *Overview map of Stockholm with endangered areas. The detailed map is shown in Figure 25.*

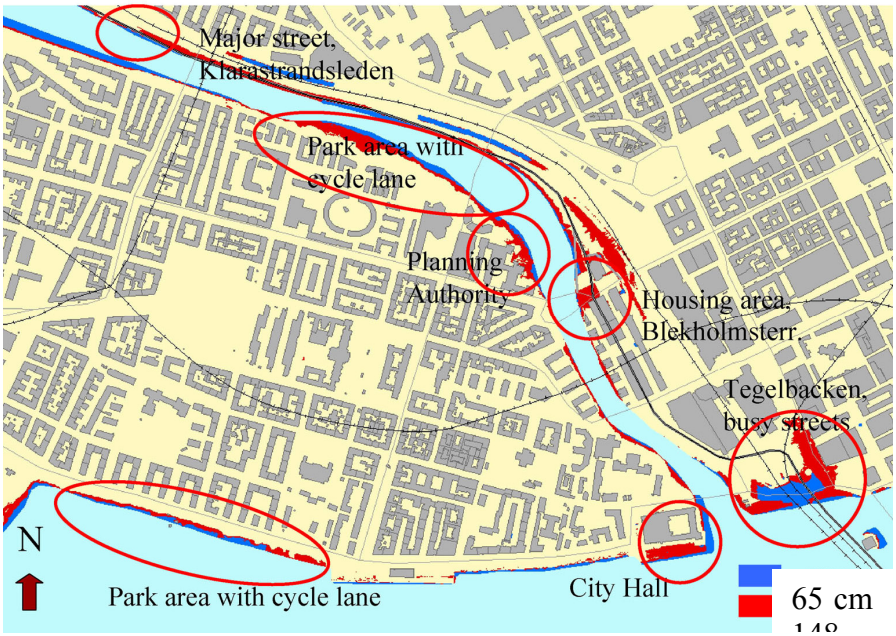

Figure 25. *Stockholm's inner city, an example of an endangered flood prone area.*

This limited assessment performed for Stockholm has been presented to local authorities. The judgement from their side is that the potential damage risks seem to be relatively small. The coping capacity of the city is regarded as high and risk management structures are considered to be well developed. An important factor is the "slow" nature of the Lake Mälaren level changes. In case the water rises, there is typically time to conduct appropriate counter measures. In this respect a local flash flood, caused by heavy rain, may flood the streets very quickly and cause major disruption to infrastructure. On the other hand, a flash flood has a

short lifetime, and passes by with main disturbances during normally a few days. A major flooding of Lake Mälaren may cause disturbances for a much longer period.

Another important issue is the possible impact on water quality after flooding. Experience from flooding events show that most damage is caused by the pollutants dissolved in the water, not the water itself. Stockholm is an old city and it became clear during this study that not much is known about contaminated soil layers close to the lake. Remnants from former industrial and other activities may pollute the flooding water. Furthermore, Lake Mälaren is, as mentioned earlier in this report, the drinking water resource in the area and thus vulnerable to pollutants.

4. Dissemination

During the SEAREG project many efforts were put into co-operation with concerned regional and municipal stakeholders, with focus on spatial planners. The work had several practical orientations:

- production of regional and municipal flood risk maps,
- raising the awareness among planners and decision makers concerning flooding risks,
- maximizing the usefulness of the project's results in the region through answering concrete demands,
- spreading information about the results among various actors, i.e. spatial planners, risk managers and technical administrators, to include flooding issues in ongoing work processes and plans,
- communication of climate modeling and flood-risk results through newsletters, seminars, presentations at conferences and result discussions with concerned actors. Direct dialogue was made with regional and local planners. For instance, the mapping results and their interpretation were discussed with groups of municipal experts, who validated the GIS-based results or disapproved them.

Crucial roles were played by the planning related actors of the county administrative boards, the Office of Regional Planning and Urban Transportation, and both selected municipalities. These partners made elevation and other data available, gave feedback about their needs, shared their experiences with the project members and gave valuable input on the results of the analysis. The work followed a dissemination plan, which was drawn up in the beginning of the project.

A particularly important outlet for disseminating information about the project and its findings was the Lake Mälaren Flooding Group, where SEAREG results were presented and discussed on several occasions. The group's work is based on voluntary co-operation between a wide range of actors who are concerned about flooding risks and actual flooding events. The group was founded after the exceptional year 2000 autumn flood of Lake Mälaren when a high water level affected and threatened various areas as well as important infrastructure around the lake. Deputies from the following bodies are members of the group: county administrative boards, county councils, municipalities (risk managers, planners, and fire brigade), water enterprises and regulators, other companies like ports, transport authorities, fishing organisations, police and military, the Swedish Meteorological and Hydrological Institute (SMHI), shipping authority, rescue authorities and services. The current numbers of partners is approximately 50.

The Lake Mälaren Flooding Group is co-ordinated by the five county administrative boards around the lake under the lead of the County Administrative Board in Stockholm. Major objectives are to prevent future flooding events, limit damages to persons, capital values and the environment, improve the exchange of information and collaboration of the concerned stakeholders, work for an extended outflow capacity from Lake Mälaren, and improve the water quality of Lake Mälaren.

Four project newsletters were also used to spread SEAREG results (SEAREG, 2004a; 2004b; 2004c; 2005). The newsletters contributed to reach decision makers with the latest ongoing results of the SEAREG project.

5. Discussion

The presented climate change projections of winds, water levels, and regional discharges are subject to various uncertainties due to natural variability, the unknown future emission of greenhouse gases, and model shortcomings. As the time slices of the simulations for present and future climate are rather long (i.e. 30 years for RCAO, 27 years for HBV, and 96 years for RCO), the uncertainty of calculated changes of mean and extreme variables is estimated to be smaller than the other uncertainties applying common tests of statistical significance. In this study only two emission scenarios (A2 and B2) were considered, which does not cover the whole range of uncertainty on plausible emission scenarios (Nakićenović et al., 2000). Consequently, the final uncertainty is also underestimated in this study. In addition, uncertainties from the models need to be considered (here: two GCMs, one RCM, oceanographical and hydrological models, DEMs). Although the impact models on regional and local scales are also biased, the largest uncertainties of the projections are likely connected to shortcomings of the GCMs. In this study lateral boundary data of two global models, HadAM3H and ECHAM4/OPYC3, were used. They implied rather different changes of large-scale circulation patterns. Thus, projected future wind fields differed considerably. In HadAM3H the area averaged changes were mostly not statistically significant whereas in ECHAM4/OPYC3 the wind speed in winter increased significantly. Interpretation of the results of this study should take all the mentioned uncertainties into account.
The hydrological work focused on investigating the effects of changed climate on the water levels in Lake Mälaren by examining a specific inflow event in detail. Using a combination of hydrological modeling and lake discharge modeling, simulations of the expected response could be made. The results present a depiction of how this observed event would vary given the changes in climate simulated by future scenarios. This does not represent the most extreme inflows that can occur within the Mälaren basin as no attempt was made here to specifically represent either the 100-year flood event or the maximum probable flood.

Looking at the characteristics of inflows during the year 2000 event, results from the hydrological analyses indicate that this type of high flow event occurring in autumn will likely become more common with the future climate. Results of both the change in the pattern of mean inflow and the change in magnitude of autumn 100-year inflows suggest this. This means that even if the magnitude of the annual 100-year inflow decreases, as is the case for all four scenarios, the risk for flooding events can still increase due to increased autumn inflows.

Of more importance than the actual magnitude of peak inflows is how long inflows of relatively high magnitude are sustained, as it is the total inflow volume over a given period that can give rise to lake flooding. Table 8 illustrates that inflow volumes are projected to be

higher in the cold season than in spring, as mean inflow rates will be higher. A compounding effect is that as autumn and winter progress, temperatures drop and evapotranspiration from both Lake Mälaren and upstream lakes will tend to decrease at the same time as increased inflows are expected.

The reference period used here for hydrological analyses is 1964-1990 and corresponds with the current standard reference period 1961-1990. As time progresses, this commonly accepted standard period is becoming the past. A look at the more recent period of 1991-2002 showed considerable deviation in mean inflow to Lake Mälaren, as compared to the reference period. Although it is not possible to confirm whether this depends on climate change or simply lies within natural variability, it is interesting to note that especially the trend of recent years resembles the characteristics of the winter period projected by climate change scenarios towards the end of the century. For the summer period the future projected decreasing inflow has not been experienced during the 1964-2002 period.

Looking at high water levels during the year 2000 event, the lake discharge modeling results confirm that under actual operations it was necessary to deviate from the Water Court Decree to maintain desired water levels. Had this not been done, the water level in Lake Mälaren would have risen another 5 cm (478 cm), as shown in Figure 18. Had the sea level been higher, the Lake Mälaren level could have risen an additional 5 cm to a total of 10 cm (483 cm) above that observed. This corresponds to a level that exceeds the present-day estimated 100-year flood level (480 cm) by 3 cm.

Considering simulations for the future climate, following the relaxed operating rules used during the actual year 2000 event would still result in higher water levels than desired, by some 5 cm (478 cm) for the RCAO-H/A2 scenario simulation and some 47 cm (520 cm) for the RCAO-E/A2 scenario simulation (Fig. 19). A coincident rise in sea level would increase these values to 17 cm (490 cm) and 54 cm (527 cm), respectively, as shown in Figure 20. These levels exceed the present-day estimated 100-year flood level, but are still far below the estimated level for the maximum probable flood.

It was possible to keep the water level of Lake Mälaren from exceeding the target level of 470 cm by assuming an increase in discharge capacity together with modifications to the operating rules specified in the Water Court Decree, as presented in Figure 21. For these lake discharge simulations, the maximum total outflow required was 930 m^3s^{-1} and 1240 m^3s^{-1} for the RCAO-H/A2 and RCAO-E/A2 scenario simulations, respectively. In relative terms, additional outflow of some 70 m^3s^{-1} was required for the RCAO-H/A2 scenario simulation and some 340 m^3s^{-1} for the RCAO-E/A2 scenario simulation. The effect of higher sea level corresponding at the same time would inhibit outflow, which implies that even larger capacity would be required to achieve the same result. For comparison, a proposed increase in capacity to 1370 m^3s^{-1} is currently under evaluation by the Ports of Stockholm. Again, it is pointed out that these numbers only correspond to this specific event, which is of lower magnitude than both the 100-year and maximum probable flood events.

The two future climate projections used here represent realizations of the same SRES-A2 emissions scenario as specified by the IPCC. Differences in the two originate primarily from model differences in the two GCMs used to generate the global projections. Both are state of the art models and it is not currently possible to determine if one is more likely to occur than the other. Thus, these differences represent the range of uncertainty currently associated with studies of this kind. There is, in addition, uncertainty originating from the hydrological

modeling. Examination of hydrological simulation results for present day conditions of the year 2000 event showed some underestimation of inflows. This indicates that the scenario inflows could also tend to be underestimated in the hydrological model. In other words, the increased inflows from the changed climate may represent the lower bound of uncertainty and future inflows could be even higher than indicated here.

As mentioned above, no attempt was made here to re-calculate how climate change may affect the design floods that form the basis for extremes used in existing floodplain mapping. Such calculations are not trivial to perform and were outside the scope of this study. However, studies to examine such extremes are of great importance in evaluating future risks for flooding. They would provide critical inputs for additional analyses to quantify needs for increased outflow capacity from the lake.

During the GIS work several problems occurred that relate to adaptability, accuracy, reliability, and usability. Each municipality uses its own system of elevation data which makes the analysis by an external user complicated as each analysis needs its own adapted GIS-platform. Regional elevation data are only useful for general analysis, and even the municipalities' elevation data must be regarded critically in part due to insufficient accuracy. As often, GIS data alone reflect only an `electronic´ truth, local surveys and discussions with local planners must complement the results of the DEMs. The results achieved should be included in planning activities, where usage is dependent on the quality of the in-data and acceptance from the responsible planners. Plausible changes in land use during the century should also be included in a local analysis on effected land.

In Sweden today, there is a trend towards establishing housing areas close to water courses and lakes. Most of the municipalities in the Mälaren region plan and build new construction quite close to the water. This may lead to a higher vulnerability to flooding. Stockholm's comprehensive plan from year 1999 does not mention flood risks. As no major flood events occurred since the start of the regulation of the Lake Mälaren, within the city's various administrations flooding has no priority. So far flooding is not a part of the planning routines, but is recognized as important to include.

At Ekerö new housing areas are suggested in very low-lying areas near the water (comprehensive plan from year 2004). Examples of new building sites are Gallstaö, Northern Tappström, and eastwards of Ekerö centrum, (see Figure 23). The risk margin of the municipality for flooding is 1.6 m above the mean water level, i.e. 0.1 m higher than the anticipated maximum probable flood level. New detailed plans contain regulations that take this margin into account. Moreover, the municipality together with the road authority works to adapt the road network of the islands so that embankments would withstand coming flooding events.

Water level limits specified by the Water Court Decree (between 415 and 470 cm in the Mälaren reference system) are important preconditions for many sectors as for instance the harbors, the water supply, the inland water shipping and not at least for real estate owners. The supervision of Lake Mälaren's water level is therefore important for many stakeholders in the region.

6. Conclusions

A dynamical downscaling technique has been successfully applied to calculate surface wind fields over sea, water levels in the Baltic Sea and Lake Mälaren, and flood prone areas in two selected municipalities in the Lake Mälaren region. Surface winds of the RCM were not used to calculate storm surges because in the control simulations both mean wind speed and wind speed extremes are underestimated compared to observations at the Landsort station. We found that the mean wind speed biases are caused partly by biases of the lateral boundary data of the GCMs whereas the underestimation of high wind speed is a general problem of state-of-the-art RCMs when no gust parameterization is used.

In the scenario simulations driven by ECHAM4/OPYC3 area averaged wind speed increases significantly during all seasons except summer when there is a significant decrease. The increase in wind speed in wintertime is a result of a stronger north-south pressure gradient in the scenario simulations. This means that also the wind direction becomes more westerly during these seasons. In the scenario simulations driven by HadAM3H the changes are much smaller and mostly not statistically significant. In all four scenario simulations the largest increases during winter and spring were found in the Gulf of Bothnia and Gulf of Finland caused by changes of the sea ice cover. In all scenario simulations absolute changes of mean and extreme wind speeds are similar.

In the hindcast simulation for 1903-1998 sea level extremes are in good agreement with observations and not systematically underestimated because the wind forcing was calculated from SLP fields. In the four scenario simulations the changes of sea level extremes differ considerably following the changes of wind speed. In the ECHAM4/OPYC3 driven scenario simulations sea level extremes increase significantly with largest changes in the eastern Baltic, i.e. Gulf of Finland and Gulf of Riga. These changes are larger than the changes of the mean sea level. In the HadAM3H driven scenario simulations the changes of the extreme sea levels are much smaller (as found for the mean sea levels) and only statistically significant in RCO-H/A2 in the northern and eastern Baltic.

In the ECHAM4/OPYC3 driven scenario simulations the magnitude of wind induced changes of sea level extremes is in most areas comparable to the land uplift and the global average sea level rise. Taking all three factors (regional wind change, land uplift, and global sea level rise) into account we found that the largest changes of sea level extremes will occur on the eastern and southeastern coasts of the Baltic proper, Gulf of Riga, and Gulf of Finland. In the eastern Gulf of Bothnia the largest wind induced changes together with the largest global sea level rise are almost compensated by land uplift. Also in Stockholm the risk of flooding from sea level changes is relatively small because in all projections the critical height of the jetty walls will not be exceeded.

Looking at Lake Mälaren, valuable tools have been developed from this work that can assist in planning for both present and future operations of the lake water level. The lake discharge model provides a tool that represents both the physical and legal structures of regulation from Lake Mälaren and can be used to further evaluate projections of changes in the physical structures as well as modifications to operating rules.

Some specific conclusions concerning Lake Mälaren and high flow situations can be made. Future climate scenario simulations indicate increased runoff inflow to Lake Mälaren during autumn and winter, and decreased inflow during spring and summer. Increased sea level in

the Baltic can influence water levels in the lake; however increased hydrological inflows show a greater impact on lake water levels than increases in sea level. Changes in climate will likely require modifications to the operating rules for regulating the lake. Furthermore, an identified need for increased discharge capacity from the lake for the present climate does not diminish with scenarios of future climate change. The decreased scenario inflow to Lake Mälaren during summer as well as the prolonged summer period probably increases the risk of a water level below the stipulated minimum level. This may cause problems to shipping and also a deteriorated water quality during summer.

The production of a series of GIS maps and related analysis, several workshops, seminars and discussion rounds with participants from all parts of the Lake Mälaren region led to the understanding, that an assessment of flood risks should find application in the design of municipal plans, regional supervision of local plans and risk management. An interdisciplinary discussion of potential risks is necessary in order to estimate the vulnerability of a municipality.

Many new housing projects along the waterfronts make thorough risk analysis indispensable. The use of cost and benefit terms in the assessments would be important for planners and decision makers. However, identification, quantification and valuation of damages and adaptation measures associated to future flooding risks is difficult.

Acknowledgements

This work was performed in part within the SEAREG project with funding from the EU Baltic Sea Region INTERREG IIIB and from the Swedish Meteorological and Hydrological Institute (SMHI). Special recognition is given to Lennart Hedin (SMHI) for providing an initial program of the hydraulics equations, to Carl Granström (SMHI) for assisting in additional development of the lake discharge model, and to Karin Larsson (Inregia AB) and Johan Stålnacke (Inregia AB) for producing the GIS maps. The authors would also like to acknowledge the Ports of Stockholm for valuable assistance in understanding the operations of Lake Mälarens regulation system, the City of Stockholm for making data available, and both the municipality of Ekerö and the City of Stockholm for a good co-operation within the SEAREG project.

References

Alenius, P., Myberg, K. & Nekrasov, A. 1998. The physical oceanography of the Gulf of Finland: a review. Boreal Environ. Res. 3, 97-125.

Andréasson, J., Bergström, S., Carlsson, B., Graham, L.P. & Lindström, G. 2004. Hydrological change - climate change impact simulations for Sweden. Ambio 33(4-5), 228-234.

Arheimer, B., Andréasson, J., Fogelberg, S., Johnsson, H., Pers, C.B. & Persson, K. 2005. Climate change impact on water quality: Model results from southern Sweden. Ambio 34(7), 559-566.

Arheimer, B. & Brandt, M. 1998. Modelling nitrogen transport and retention in the catchments of southern Sweden. Ambio 27(6), 471-480.

Arnell, N.W. 1998. Climate change and water resources in Britain. Climatic Change 39, 83-110.

Baerens, C. & Hupfer, P. 1999. Extremwasserstände an der deutschen Ostseeküste nach Beobachtungen und in einem Treibhausgasszenario. Die Küste 61, 47-72.

Bergström, S. 1995. The HBV Model. In: V.P. Singh (ed.), Computer Models of Watershed Hydrology. Water Resources Publications, Highlands Ranch, Colorado, 443-476.

Bergström, S., Andréasson, J., Beldring, S., Carlsson, B., Graham, L.P., Jónsdóttir, J.F., Engeland, K., Turunen, M.A., Vehviläinen, B. & Førland, E.J. 2003. Climate Change Impacts on Hydropower in the Nordic Countries - State of the art and discussion of principles. CWE Report no. 1, CWE Hydrological Models Group, Rejkjavik, Iceland, 36 pp.

Bergström, S., Carlsson, B., Gardelin, M., Lindström, G., Pettersson, A. & Rummukainen, M. 2001. Climate change impacts on runoff in Sweden - assessments by global climate models, dynamical downscaling and hydrological modelling. Climate Research 16(2), 101-112.

Church, J.A., Gregory, J.M., Huybrechts, P., Kuhn, M., Lambeck, K., Nhuan, M.T., Qin, D. and Woodworth, P. 2001. Changes in Sea Level. In: Houghton J.T. et al. (eds.), Climate Change 2001: The scientific basis. Contribution of Working Group I to the Third Assessment Report of the Intergovernmental Panel on Climate Change, Cambridge University Press, Cambridge, United Kingdom and New York, NY, USA, 639-693.

Döscher, R., Willén, U., Jones, C., Rutgersson, A., Meier, H.E.M., Hansson, U. & Graham, L.P. 2002. The development of the regional coupled ocean-atmosphere model RCAO. Boreal Environment Research 7(3), 183-192.

Döscher, R. & Meier, H.E.M. 2004. Simulated sea surface temperature and heat fluxes in different climates of the Baltic Sea. Ambio 33, 242-248.

Ehlert, K. 1970. Mälarens hydrologi och inverkan på denna av alternativa vattenavledningar från Mälaren (The hydrology of Lake Mälaren and influencing effects from alternative water

releases, in Swedish). SMHI Rapporter Hydrologi, nr 8, Swedish Meteorological and Hydrological Institute, Norrköping, Sweden.

Ekman, M. 1996. A consistent map of the postglacial uplift of Fennoscandia. Terra Nova, 8, 158-165.

Ekman, M., & Mäkinen, J. 1995. Mean Sea Surface Topography in a Unified Height System for the Baltic Sea Area. In Proceedings, Coordinate Systems, GPS, and the Geoid. June 27-29, 1994, Espoo, Finland. (Ed. M. Vermeer) Reports of the Finnish geodetic Institute, 95:4, 53-62
Gardelin, M., Bergström, S., Carlsson, B., Graham, L.P. & Lindström, G. 2002. Climate Change and Water Resources in Sweden - Analysis of Uncertainties. In: M. Beniston (ed.), Climatic Change: Implications for the Hydrological Cycle and for Water Management. Advances in Global Change Research. Kluwer Academic Publishers, Dordrecht, 189-207.

Gellens, D. & Roulin, E. 1998. Streamflow response of Belgian catchments to IPCC climate change scenarios. Journal of Hydrology 210, 242-258.

Gibson, J.K., Kållberg, P., Uppala, S., Nomura, A., Hernandez, A. and Serrano, E., 1997. ERA description. ECMWF Re-analysis Final Report Series 1, 71pp.

Gordon, C., Cooper, C., Senior, C.A., Banks, H., Gregory, J.M., Johns, T.C., Mitchell, J.F.B., & Wood, R.A. 2000. The simulation of SST, sea ice extent and ocean heat transports in a version of the Hadley Centre coupled model without flux adjustments. Clim. Dyn. 16, 147-166.

Graham, L.P. 2004. Climate change effects on river flow to the Baltic Sea. Ambio 33(4-5), 235-241.

Hupfer, P., Harff, J., Sterr, H., Stigge, H.-J. (ed.) 2003. Die Wasserstände an der Ostseeküste: Entwicklung – Sturmfluten – Klimawandel. Die Küste 66, 331 pp.

Jones, C.G., Ullerstig, A., Willén, U. & Hansson, U. 2004. The Rossby Centre regional atmospheric climate model (RCA). Part I: Model climatology and performance characteristics for present climate over Europe. Ambio 33, 199-210.

Jones, R.G., Murphy, J.M., Hassell, D.C. & Woodage, M.J. 2006. A high resolution atmospheric GCM for the generation of regional climate scenarios. Clim. Dyn., submitted.

Kalnay, E., Kanamitsu, M., Kistler, R., Collins, W., Deaven, D., Gandin, L., Iredell, M, Saha, S., White, G., Woollen, J., Chelliah, M., Zhu, Y., Ebisuzaki, W., Higgins, W., Janowiak, J., Mo, K.C., Ropelweski, C., Wand, J., Leetma, A., Reynolds, R., Jenne, R. & Joseph, D. 1996. The NCEP/NCAR 40 reanalysis project. Bull. Am. Met. Soc. 77, 437-471.

Kauker, F. & Meier, H.E.M. 2003. Modeling decadal variability of the Baltic Sea: 1. Reconstructing atmospheric surface data for the period 1902-1998. J. Geophys. Res., 108(C8), 3267.

Kistler, R., Kalnay, E., Collins, W., Saha, S., White, G., Woollen, J., Chelliah, M., Ebisuzaki, W., Kanamitsu, M., Kousky, V., van den Dool, H., Jenne, R. & Fiorino, M. 2001. The NCEP-

NCAR 50 year reanalysis: Monthly mean CD-ROM and documentation. Bull. Am. Met. Soc. 82, 247-267.

Kjellström, E. 2004. Recent and future signatures of climate change in Europe. Ambio 33, 193-198.

Lindström, G. 1997. A Simple Automatic Calibration Routine for the HBV Model. Nordic Hydrology, 28, 153-168.

Lindström, G., Johansson, B., Persson, M., Gardelin, M. & Bergström, S. 1997. Development and test of the distributed HBV-96 model. Journal of Hydrology 201, 272-288.

Meier, H.E.M. 2006. Baltic Sea climate in the late 21st century – a dynamical downscaling approach using two global models and two emission scenarios. Climate Dynamics, in press.

Meier, H.E.M. & Kauker, F. 2003. Modeling decadal variability of the Baltic Sea: 2. Role of freshwater inflow and large-scale atmospheric circulation for salinity. J. Geophys. Res., 108(C11), 3368.

Meier, H.E.M., Broman, B. & Kjellström, E. 2004a. Simulated sea level in past and future climates of the Baltic Sea. Climate Research 27, 59-75.

Meier, H.E.M., Döscher, R. & Faxén, T. 2003. A multiprocessor coupled ice-ocean model for the Baltic Sea: Application to the salt inflow. J. Geophys. Res. 108(C8), 3273, doi:10.1029/2000JC000521.

Meier, H.E.M., Döscher, R. & Halkka, A. 2004b. Simulated distributions of Baltic sea-ice in warming climate and consequences for the winter habitat of the Baltic ringed seal. Ambio 33, 249-256.

Middelkoop, H., Daamen, K., Gellens, D., Grabs, W., Kwadijk, J.C.J., Lang, H., Parmet, B.W.A.H., Schädler, B., Schulla, J. & Wilke, K. 2001. Impact of climate change on hydrological regimes and water resources management in the Rhine Basin. Climatic Change 49, 105-128.

Nakićenović, N., Alcamo, J., Davis, G., de Vries, B., Fenhann, J., Gaffin, S., Gregory, K., Grübler, A., Jung, T.Y., Kram, T., La Rovere, E.L., Michaelis, L., Mori, S., Morita, T., Pepper, W., Pitcher, H., Price, L., Riahi, K., Roehrl, A., Rogner, H.-H., Sankovski, A., Schlesinger, M., Shukla, P., Smith, S., Swart, R., van Rooijen, S., Victor, N. & Dadi, Z. 2000. Emission scenarios. A Special Report of Working Group III of the Intergovernmental Panel on Climate Change. Cambridge University Press, 599 pp.

Nash, J.E. & Sutcliffe, J.V. 1970. River flow forecasting through conceptual models part I - A discussion of principles. Journal of Hydrology 10, 282-290.

New, M., Hulme, M. & Jones, P. 1999. Representing twentieth-century space-time climate variability. Part I: Development of a 1961-90 mean monthly terrestrial climatology. J. Clim. 12, 829-856.

New, M., Hulme, M. & Jones, P. 2000. Representing twentieth-century space-time climate variability. Part II: Development of 1901-96 monthly grids of terrestrial surface climate. J. Clim. 13, 2217-2238.

Pope, D.V., Gallani, M., Rowntree, R. & Stratton, A. 2000. The impact of new physical parameterizations in the Hadley Centre climate model: HadAM3. Clim. Dyn. 16, 123-146.

Press, W.H., Teukolsky, S.A., Vetterling, W.T. & Flannery, B.P. 1999. Numerical recipes in Fortran 77: The art of scientific computing, 933 pp.

Pryor, S.P. & Barthelmie, R.J. 2004. Use of RCM simulations to assess the impact of climate change on wind energy availability. Risø-R-1477(EN). Risø National Laboratory, Roskilde, Danmark. ISBN 87-550-3368-7, 111 p.

Pryor, S.P., Barthelmie, R.J. & Kjellström, E. 2005. Potential climate change impact on wind energy resources in northern Europe: analyses using a regional climate model. Clim. Dyn. 25, 815-835.

Rockel, B. 2004. Near surface wind speed extremes over Europe in PRUDENCE control and scenario simulations of eight RCMs. In: L. Bärring and R. Laprise (eds.) Proceedings from WCRP Workshop on Regional Climate Modelling. Lund, Sweden 29 March - 2 April 2004. *Lund eRep. Phys. Geogr*., No. 5, May 2005.

Rockel, B. & Woth, K. 2005. Future changes in near surface wind speed extremes over Europe from an ensemble of RCM simulations. *Clim. Change*, submitted.

Roeckner, E., Bengtsson, L., Feichter, J., Lelieveld, J. & Rodhe, H. 1999. Transient climate change simulations with a coupled atmosphere-ocean GCM including the tropospheric sulfur cycle. Journal of Climate 12, 3004-3032.

Räisänen, J., Hansson, U., Ullerstig, A., Döscher, R., Graham, L.P., Jones, C., Meier, M., Samuelsson, P. & Willén, U. 2003. GCM driven simulations of recent and future climate with the Rossby Centre coupled atmosphere – Baltic Sea regional climate model RCAO, RMK No 101, SMHI, SE 60176 Norrköping, Sweden, 61 pp.

Räisänen, J., Hansson, U., Ullerstig, A., Döscher, R., Graham, L.P., Jones, C., Meier, H.E.M., Samuelsson, P. & Willén, U. 2004. European climate in the late twenty-first century: regional simulations with two driving global models and two forcing scenarios. Climate Dynamics 22, 13-31.

SEAREG 2004a. Nyhetsbrev Årgång 1 Nummer 1, January 2004. Available from http://www.smhi.se/sgn0106/if/rc/projects/SEAREG.html.

SEAREG 2004b. Nyhetsbrev Årgång 1 Nummer 2, May 2004. Available from http://www.smhi.se/sgn0106/if/rc/projects/SEAREG.html.

SEAREG 2004c. Nyhetsbrev Årgång 1 Nummer 3, November 2004. Available from http://www.smhi.se/sgn0106/if/rc/projects/SEAREG.html.

SEAREG 2005. Nyhetsbrev Årgång 2 Nummer 1, March 2005. Available from

http://www.smhi.se/sgn0106/if/rc/projects/SEAREG.html.

Schmidt-Thome, P. (editor) 2006. Sea level Changes Affecting the Spatial Development of the Baltic Sea Region, Geological Survey of Finland, Special Paper 41, Espoo, in press.

SRV 2001. Översiktlig översvämningskartering för Mälaren (Overview maps of floodplain extent for Lake Mälaren, in Swedish). SRV Rapport, nr. 22, Swedish Rescue Services, Karlstad, Sweden, 27 pp.

Uppala, S.M., Kållberg, P.W., Simmons, A.J., Andrae, U., da Costa Bechtold, V., Fiorino, M., Gibson, J.K., Haseler, J., Hernandez, A., Kelly, G.A., Li, X., Onogi, K., Saarinen, S., Sokka, N., Allan, R.P., Andersson, E., Arpe, K., Balmaseda, M.A., Beljaars, A.C.M., van de Berg, L., Bidlot, J., Bormann, N., Caires, S., Chevallier, F., Dethof, A., Dragosavac, M., Fisher, M., Fuentes, M., Hagemann, S., Hólm, E., Hoskins, B.J., Isaksen, L., Janssen, P.A.E.M., Jenne, R., McNally, A.P., Mahfouf, J.-F., Morcrette, J.-J., Rayner, N.A., Saunders, R.W., Simon, P., Sterl, A., Trenberth, K.E., Untch, A., Vasiljevic, D., Viterbo, P. & Woollen, J. 2005. The ERA-40 Reanalysis. Quart. J. R. Meteorol. Soc., 131, 2961-3012, doi:10.1256/qj.04.176.

Vehviläinen, B. & Huttunen, M. 1997. Climate change and water resources in Finland. Boreal Environment Research 2, 3-18.

Wilks, D.S. 1995. Statistical methods in the atmospheric sciences. Academic Press, London, 467 pp.

Appendix: List of abbreviations

ANN	Annual
AOGCM	Atmosphere Ocean General Circulation Model
BSR	Baltic Sea Region
CRU	Climate Research Unit
CRU TS 1.0	Climate Research Unit Time Series version 1.0
DEM	Digital Elevation Model
DJF	December, January, February
ECHAM4/OPYC3	A GCM from the Max Planck Institute for Meteorology in Hamburg, Germany
ECMWF	European Center for Medium range Weather Forecasting
ERA15	ECMWF Re-Analysis December 1978 to February 1994
ERA40	ECMWF Re-Analysis September 1957 to August 2001
EU	European Union
FAR	False Alarm Ratio
GCM	General Circulation Model or Global Climate Model
GIS	Geographical Information System
HadAM3H	A GCM from the Hadley Centre in UK
HBV	SMHI hydrological model
IPCC	Intergovernmental Panel on Climate Change
JJA	June, July, August
MAM	March, April, May
MPF	Maximum probable flood
NCEP	National Centers for Environmental Protection
NH60	Nordic Height system 1960
POD	Probability Of Detection
RCA2	Rossby Centre Atmosphere Model version 2
RCA2-ERA15	RCA2 forced by ERA15-data
RCAO	Rossby Centre Atmosphere Ocean Model or Rossby Centre regional climate model
RCAO-E	RCAO driven by ECHAM4/OPYC3, control simulation
RCAO-E/A2	RCAO driven by ECHAM4/OPYC3 with SRES A2 forcing
RCAO-E/B2	RCAO driven by ECHAM4/OPYC3 with SRES B2 forcing
RCAO-H	RCAO driven by HadAM3H, control simulation
RCAO-H/A2	RCAO driven by HadAM3H with SRES A2 forcing
RCAO-H/B2	RCAO driven by HadAM3H with SRES B2 forcing
RCM	Regional Climate Model
RCO	Rossby Centre Ocean model or Rossby Centre coupled ice-ocean model
RCO-E/A2	RCO driven by RCAO-E/A2
RCO-E/B2	RCO driven by RCAO-E/B2
RCO-H/A2	RCO driven by RCAO-H/A2
RCO-H/B2	RCO driven by RCAO-H/B2
RCO-REF	RCO reference run 1903-1998
RH70	Height reference system
SEAREG	Sea Level Change Affecting the Spatial Development in the Baltic Sea Region
SLP	Sea Level Pressure
SMHI	Swedish Meteorological and Hydrological Institute
SON	September, October, November
SRES A2, B2	Emission scenarios from the IPCC Special Report (2000)
SST	Sea Surface Temperature
SYNOP station	Synoptic station
TSS	True Skill Score

SMHI Publications

SMHI publishes six report series. Three of these, the R-series, are intended for international readers and are in most cases written in English. For the others the Swedish language is used.

Names of the Series	Published since
RMK (Report Meteorology and Climatology)	1974
RH (Report Hydrology)	1990
RO (Report Oceanography)	1986
METEOROLOGI	1985
HYDROLOGI	1985
OCEANOGRAFI	1985

Earlier issues published in serie RMK

1 Thompson, T., Udin, I. and Omstedt, A. (1974)
Sea surface temperatures in waters surrounding Sweden.

2 Bodin, S. (1974)
Development on an unsteady atmospheric boundary layer model.

3 Moen, L. (1975)
A multi-level quasi-geostrophic model for short range weather predictions.

4 Holmström, I. (1976)
Optimization of atmospheric models.

5 Collins, W.G. (1976)
A parameterization model for calculation of vertical fluxes of momentum due to terrain induced gravity waves.

6 Nyberg, A. (1976)
On transport of sulphur over the North Atlantic.

7 Lundqvist, J.-E. and Udin, I. (1977)
Ice accretion on ships with special emphasis on Baltic conditions.

8 Eriksson, B. (1977)
Den dagliga och årliga variationen av temperatur, fuktighet och vindhastighet vid några orter i Sverige.

9 Holmström, I., and Stokes, J. (1978)
Statistical forecasting of sea level changes in the Baltic.

10 Omstedt, A. and Sahlberg, J. (1978)
Some results from a joint Swedish-Finnish sea ice experiment, March, 1977.

11 Haag, T. (1978)
Byggnadsindustrins väderberoende, seminarieuppsats i företagsekonomi, B-nivå.

12 Eriksson, B. (1978)
Vegetationsperioden i Sverige beräknad från temperaturobservationer.

13 Bodin, S. (1979)
En numerisk prognosmodell för det atmosfäriska gränsskiktet, grundad på den turbulenta energiekvationen.

14 Eriksson, B. (1979)
Temperaturfluktuationer under senaste 100 åren.

15 Udin, I. och Mattisson, I. (1979)
Havsis- och snöinformation ur datorbearbetade satellitdata - en modellstudie.

16 Eriksson, B. (1979)
Statistisk analys av nederbördsdata. Del I. Arealnederbörd.

17 Eriksson, B. (1980)
Statistisk analys av nederbördsdata. Del II. Frekvensanalys av månadsnederbörd.

18 Eriksson, B. (1980)
Årsmedelvärden (1931-60) av nederbörd, avdunstning och avrinning.

19 Omstedt, A. (1980)
A sensitivity analysis of steady, free floating ice.

20 Persson, C. och Omstedt, G. (1980)
En modell för beräkning av luftföroreningars spridning och deposition på mesoskala.

21 Jansson, D. (1980)
Studier av temperaturinversioner och vertikal vindskjuvning vid Sundsvall-Härnösands flygplats.

22 Sahlberg, J. and Törnevik, H. (1980)
A study of large scale cooling in the Bay of Bothnia.

23 Ericson, K. and Hårsmar, P.-O. (1980)
Boundary layer measurements at Klock-rike. Oct. 1977.

24 Bringfelt, B. (1980)
A comparison of forest evapotranspiration determined by some independent methods.

25 Bodin, S. and Fredriksson, U. (1980)
Uncertainty in wind forecasting for wind power networks.

26 Eriksson, B. (1980)
Graddagsstatistik för Sverige.

27 Eriksson, B.(1981)
Statistisk analys av nederbördsdata. Del III. 200-åriga nederbördsserier.

28 Eriksson, B. (1981)
Den "potentiella" evapotranspirationen i Sverige.

29 Pershagen, H. (1981)
Maximisnödjup i Sverige (perioden 1905-70).

30 Lönnqvist, O. (1981)
Nederbördsstatistik med praktiska tillämpningar.
(Precipitation statistics with practical applications.)

31 Melgarejo, J.W. (1981)
Similarity theory and resistance laws for the atmospheric boundary layer.

32 Liljas, E. (1981)
Analys av moln och nederbörd genom automatisk klassning av AVHRR-data.

33 Ericson, K. (1982)
Atmospheric boundary layer field experiment in Sweden 1980, GOTEX II, part I.

34 Schoeffler, P. (1982)
Dissipation, dispersion and stability of numerical schemes for advection and diffusion.

35 Undén, P. (1982)
The Swedish Limited Area Model. Part A. Formulation.

36 Bringfelt, B. (1982)
A forest evapotranspiration model using synoptic data.

37 Omstedt, G. (1982)
Spridning av luftförorening från skorsten i konvektiva gränsskikt.

38 Törnevik, H. (1982)
An aerobiological model for operational forecasts of pollen concentration in the air.

39 Eriksson, B. (1982)
Data rörande Sveriges temperaturklimat.

40 Omstedt, G. (1984)
An operational air pollution model using routine meteorological data.

41 Persson, C. and Funkquist, L. (1984)
Local scale plume model for nitrogen oxides. Model description.

42 Gollvik, S. (1984)
Estimation of orographic precipitation by dynamical interpretation of synoptic model data.

43 Lönnqvist, O. (1984)
Congression - A fast regression technique with a great number of functions of all predictors.

44 Laurin, S. (1984)
Population exposure to SO and NO_x from different sources in Stockholm.

45 Svensson, J. (1985)
Remote sensing of atmospheric tempera-ture profiles by TIROS Operational Vertical Sounder.

46 Eriksson, B. (1986)
Nederbörds- och humiditetsklimat i Sverige under vegetationsperioden.

47 Taesler, R. (1986)
Köldperioden av olika längd och förekomst.

48 Wu Zengmao (1986)
Numerical study of lake-land breeze over Lake Vättern, Sweden.

49 Wu Zengmao (1986)
Numerical analysis of initialization procedure in a two-dimensional lake breeze model.

50 Persson, C. (1986)
Local scale plume model for nitrogen oxides. Verification.

51 Melgarejo, J.W. (1986)
An analytical model of the boundary layer above sloping terrain with an application to observations in Antarctica.

52 Bringfelt, B. (1986)
Test of a forest evapotranspiration model.

53 Josefsson, W. (1986)
Solar ultraviolet radiation in Sweden.

54 Dahlström, B. (1986)
Determination of areal precipitation for the Baltic Sea.

55 Persson, C., Rodhe, H. and De Geer, L.-E. (1986)
The Chernobyl accident - A meteorological analysis of how radionucleides reached Sweden.

56 Persson, C., Robertson, L., Grennfelt, P., Kindbom, K., Lövblad, G. och Svanberg, P.-A. (1987)
Luftföroreningsepisoden över södra Sverige 2 - 4 februari 1987.

57 Omstedt, G. (1988)
An operational air pollution model.

58 Alexandersson, H. and Eriksson, B. (1989)
Climate fluctuations in Sweden 1860 - 1987.

59 Eriksson, B. (1989)
Snödjupsförhållanden i Sverige - Säsongerna 1950/51 - 1979/80.

60 Omstedt, G. and Szegö, J. (1990)
Människors exponering för luftföroreningar.

61 Mueller, L., Robertson, L., Andersson, E. and Gustafsson, N. (1990)
Meso-γ scale objective analysis of near surface temperature, humidity and wind, and its application in air pollution modelling.

62 Andersson, T. and Mattisson, I. (1991)
A field test of thermometer screens.

63 Alexandersson, H., Gollvik, S. and Meuller, L. (1991)
An energy balance model for prediction of surface temperatures.

64 Alexandersson, H. and Dahlström, B. (1992)
Future climate in the Nordic region - survey and synthesis for the next century.

65 Persson, C., Langner, J. and Robertson, L. (1994)
Regional spridningsmodell för Göteborgs och Bohus, Hallands och Älvsborgs län. (A mesoscale air pollution dispersion model for the Swedish west-coast region. In Swedish with captions also in English.)

66 Karlsson, K.-G. (1994)
Satellite-estimated cloudiness from NOAA AVHRR data in the Nordic area during 1993.

67 Karlsson, K-G. (1996)
Cloud classifications with the SCANDIA model.

68 Persson, C. and Ullerstig, A. (1996)
Model calculations of dispersion of lindane over Europe. Pilot study with comparisons to easurements around the Baltic Sea and the Kattegat.

69 Langner, J., Persson, C., Robertson, L. and Ullerstig, A. (1996)
Air pollution Assessment Study Using the MATCH Modelling System. Application to sulfur and nitrogen compounds over Sweden 1994.

70 Robertson, L., Langner, J. and Engardt, M. (1996)
MATCH - Meso-scale Atmosperic Transport and Chemistry modelling system.

71 Josefsson, W. (1996)
Five years of solar UV-radiation monitoring in Sweden.

72 Persson, C., Ullerstig, A., Robertson, L., Kindbom, K. and Sjöberg, K. (1996)
The Swedish Precipitation Chemistry Network. Studies in network design using the MATCH modelling system and statistical methods.

73 Robertson, L. (1996)
Modelling of anthropogenic sulfur deposition to the African and South American continents.

74 Josefsson, W. (1996)
Solar UV-radiation monitoring 1996.

75 Häggmark, L. Ivarsson, K.-I. and Olofsson, P.-O. (1997)
MESAN - Mesoskalig analys.

76 Bringfelt, B., Backström, H., Kindell, S., Omstedt, G., Persson, C. and Ullerstig, A. (1997)
Calculations of PM-10 concentrations in Swedish cities- Modelling of inhalable particles

77 Gollvik, S. (1997)
The Teleflood project, estimation of precipitation over drainage basins.

78 Persson, C. and Ullerstig, A. (1997)
Regional luftmiljöanalys för Västmanlands län baserad på MATCH modell-beräkningar och mätdata - Analys av 1994 års data

79 Josefsson, W. and Karlsson, J.-E. (1997)
Measurements of total ozone 1994-1996.

80 Rummukainen, M. (1997)
Methods for statistical downscaling of GCM simulations.

81 Persson, T. (1997)
Solar irradiance modelling using satellite retrieved cloudiness - A pilot study

82 Langner, J., Bergström, R. and Pleijel, K. (1998)
European scale modelling of sulfur, oxidized nitrogen and photochemical oxidants. Model development and evaluation for the 1994 growing season.

83 Rummukainen, M., Räisänen, J., Ullerstig, A., Bringfelt, B., Hansson, U., Graham, P. and Willén, U. (1998)
RCA - Rossby Centre regional Atmospheric climate model: model description and results from the first multi-year simulation.

84 Räisänen, J. and Döscher, R. (1998)
Simulation of present-day climate in Northen Europé in the HadCM2 OAGCM.

85 Räisänen, J., Rummukainen, M., Ullerstig, A., Bringfelt, B., Hansson, U. and Willén, U. (1999)
The First Rossby Centre Regional Climate Scenario - Dynamical Downscaling of CO_2-induced Climate Change in the HadCM2 GCM.

86 Rummukainen, M. (1999)
On the Climate Change debate

87 Räisänen, J. (2000)
CO_2-induced climate change in northern Europé: comparison of 12 CMIP2 experiments.

88 Engardt, M. (2000)
Sulphur simulations for East Asia using the MATCH model with meteorological data from ECMWF.

89 Persson, T. (2000)
Measurements of Solar Radiation in Sweden 1983-1998

90 Michelson, D. B., Andersson, T., Koistinen, J., Collier, C. G., Riedl, J., Szturc, J., Gjertsen, U., Nielsen, A. and Overgaard, S., (2000)
BALTEX Radar Data Centre Products and their Methodologies

91 Josefsson, W. (2000)
Measurements of total ozone 1997 – 1999

92 Andersson, T. (2000)
Boundary clear air echos in southern Sweden

93 Andersson, T. (2000)
Using the Sun to check some weather radar parameters

94 Rummukainen, M., Bergström, S., Källén, E., Moen, L., Rodhe, J. and Tjernström, M. (2000)
SWECLIM – The First Three Years

95 Meier, H. E. M. (2001)
The first Rossby Centre regional climate scenario for the Baltic Sea using a 3D coupled ice-ocean model

96 Landelius, T., Josefsson, W. and Persson, T. (2001)
A system for modelling solar radiation parameters with mesoscale spatial resolution

97 Karlsson, K.-G. (2001)
A NOAA AVHRR cloud climatology over Scandinavia covering the period 1991-2000

98 Bringfelt, B., Räisänen, J., Gollvik, S., Lindström, G., Graham, P. and Ullerstig, A., (2001)
The land surface treatment for the Rossby Centre Regional Atmospheric Climate Model - version 2 (RCA2)

99 Kauker, F. and Meier, H. E. M., (2002)
Reconstructing atmospheric surface data for the period 1902-1998 to force a coupled ocean-sea ice model of the Baltic Sea.

100 Klein, T., Bergström, R. and Persson, C. (2002)
Parameterization of dry deposition in MATCH

101 Räisänen, J., Hansson, U., Ullerstig A., Döscher, R., Graham, L. P., Jones, C., Meier, M., Samuelsson, P.and Willén, U. (2003)
GCM driven simulations of recent and future climate with the Rossby Centre coupled atmosphere - Baltic Sea regional climate model RCAO

102 Tjernström, M., Rummukainen, M., Bergström, S., Rodhe, J. och Persson, G., (2003)
Klimatmodellering och klimatscenarier ur SWECLIMs perspektiv.

103 Segersson, D. (2003)
Numerical Quantification of Driving Rain on Buildings

104 Rummukainen, M. and the SWECLIM participants (2003)
The Swedish regional climate modeling program 1996-2003. Final report.

105 Robertson, L. (2004)
Extended back-trajectories by means of adjoint equations

106 Rummukainen, M., Bergström S., Persson G., Ressner, E (2005)
Anpassningar till klimatförändringar

107 Taesler, R., Andersson, C., Nord, M (2005)
Optimizing Energy Efficiency and Indoor climate by Forecast Control of Heating Systems and Energy Management in Buildings

108 Kjellström, E., Bärring, L., Gollvik, S., Hansson, U., Jones, C., Samuelsson, P., Rummukainen, M., Ullerstig, A., Willén, U., Wyser, K., (2005)
A 140-year simulation of European climate with the new version of the Rossby Centre regional atmospheric climate model (RCA3).

Swedish Meteorological and Hydrological Institute
SE-601 76 Norrköping · Sweden
Tel +46 11 495 80 00 · Fax +46 11 495 80 01

ISSN 0347-2116